Journal of Asian Earth Sciences 185 (2019) 104054

Contents lists available at ScienceDirect

Journal of Asian Earth Sciences

journal homepage: www.elsevier.com/locate/jseaes

Rb-Sr isotopic age, S-Pb-Sr isotopic compositions and genesis of the ca. 200 Ma Yunluheba Pb-Zn deposit in NW Guizhou Province, SW China

Yong-Yong Tang[a,*], Xian-Wu Bi[a,*], Jia-Xi Zhou[b], Feng Liang[c], You-Qiang Qi[a], Cheng-Biao Leng[a], Xing-Chun Zhang[a], Hai Zhang[a,d]

[a] State Key Laboratory of Ore Deposit Geochemistry, Institute of Geochemistry, Chinese Academy of Sciences, Guiyang 550081, China
[b] School of Resource Environment and Earth Sciences, Yunnan University, Kunming 650500, China
[c] CNPC Key Laboratory of Carbonate Reservoirs, PetroChina Hangzhou Research Institute of Geology, Hangzhou 310023, China
[d] 113 Geological Brigade, Guizhou Bureau of Geology and Mineral Exploration, Liupanshui 553001, China

ARTICLE INFO

Keywords:
Ore genesis
Rb-Sr isotopic age
S-Pb-Sr isotopes
Yunluheba Pb-Zn deposit
Sichuan-Yunnan-Guizhou Pb-Zn metallogenic province, SW China

ABSTRACT

Over 400 carbonate-hosted Pb-Zn deposits in the western Yangtze block constitute the giant Sichuan-Yunnan-Guizhou (SYG) Pb-Zn metallogenic province. The majority of Pb-Zn deposits hosted in Devonian carbonates are characterized by low $\delta^{34}S$ values, causing debates on their ore genesis. To address this issue, the Yunluheba Pb-Zn deposit is chosen as a case study. Ore bodies of this deposit are hosted in middle Devonian carbonates. Ore minerals are sphalerite, galena and pyrite. Sphalerite Rb-Sr dating yields an isochron age of 206.2 ± 4.9 Ma, consistent with ages of most Pb-Zn deposits in the SYG province, arguing for a regional intensive Pb-Zn mineralization event during the late Indosinian orogeny. Sulfides have Pb isotopic compositions that form a linear trend above the average crustal Pb growth curve in the $^{207}Pb/^{204}Pb$ vs. $^{206}Pb/^{204}Pb$ plot. Moreover, Pb isotopic ratios are consistent with the Devonian to Permian carbonates' age-corrected Pb isotopic ratios, suggesting mixed crustal Pb sources with the majority of Pb derived from country rocks. Combined with initial $^{87}Sr/^{86}Sr$ ratios of sphalerite, approximately equal to $^{87}Sr/^{86}Sr_{200Ma}$ ratios of the D-P carbonates, ore-forming metals are considered to have been derived mainly from ore-hosting rocks. Sulfides' $\delta^{34}S_{CDT}$ values range mainly from −2.0‰ to 2.9‰, interpreted to be a result of mixing by syn-sedimentary pyrite originated biogenic S and thermochemically reduced S. We conclude that the Yunluheba deposit and other Pb-Zn deposits in the SYG province should belong to Mississippi Valley-type deposits.

1. Introduction

The contiguous Sichuan-Yunnan-Guizhou (SYG) Pb-Zn metallogenic province (Fig. 1) is a major part of the South China low-temperature metallogenic domain (Hu et al., 2017a, 2017b; Li, 1999; Tu, 1998) and hosts over 400 carbonate-hosted Pb-Zn deposits with metal resources of more than 26 million tons, making it an important region for base metal production in China (Hu et al., 2017a, 2017b; Liu and Lin, 1999; Zhou et al., 2018b). These Pb-Zn deposits are characterized by high grades of Pb + Zn (generally > 10%) and are enriched in a variety of elements, such as Cd, Ga, Ge and In (Li, 2003; Si et al., 2013; Wang et al., 2008). Among these deposits, the economically important deposits include those in Huize, Maoping, Daliangzi and Tianbaoshan (Shen et al., 2016; Wang et al., 2018; Yin et al., 2009; Zhang et al., 2008). Many studies consider the SYG deposits to be Mississippi Valley-type (MVT) deposits (e.g., Han et al., 2007; Hu et al., 2017b; Jin and Huang, 2008; Wang et al., 2001; Zhang et al., 2015; Zhou et al., 2001), which are generally characterized by epigenetic ore precipitated from dense basinal brines at approximately 75–200 °C, platform carbonate host rocks and no direct relationship with igneous activity (Leach and Sangster, 1993). However, other compelling perspectives have also been proposed, including Emeishan basalt-related magmatic-hydrothermal origins (Huang et al., 2004; Xu et al., 2014; Zhou et al., 2018b), sedimentary exhalation (Tang, 1999), and sedimentary reworking mineralization (e.g., Liao, 1984; Zhao, 1995). Recent geochronological work has suggested that most of the carbonate-hosted Pb-Zn deposits in the SYG province could have formed during the late Indosinian orogeny (230–190 Ma, Table 1; Li et al., 2004; Lin et al., 2010; Wu, 2013; Yin et al., 2009; Zhang et al., 2015; Zhang et al., 2015; Zhang et al., 2014; Zhou et al., 2013c; Zhou et al., 2013d; Zhou et al., 2015). Furthermore, the deposits show a general range of $\delta^{34}S$ values from 8‰ to 20‰, indicating that the S was mainly sourced from seawater sulfates in the

* Corresponding authors.
E-mail addresses: tangyongyong@vip.gyig.ac.cn (Y.-Y. Tang), bixianwu@vip.gyig.ac.cn (X.-W. Bi).

https://doi.org/10.1016/j.jseaes.2019.104054
Received 30 March 2019; Received in revised form 21 September 2019; Accepted 29 September 2019
Available online 30 September 2019
1367-9120/

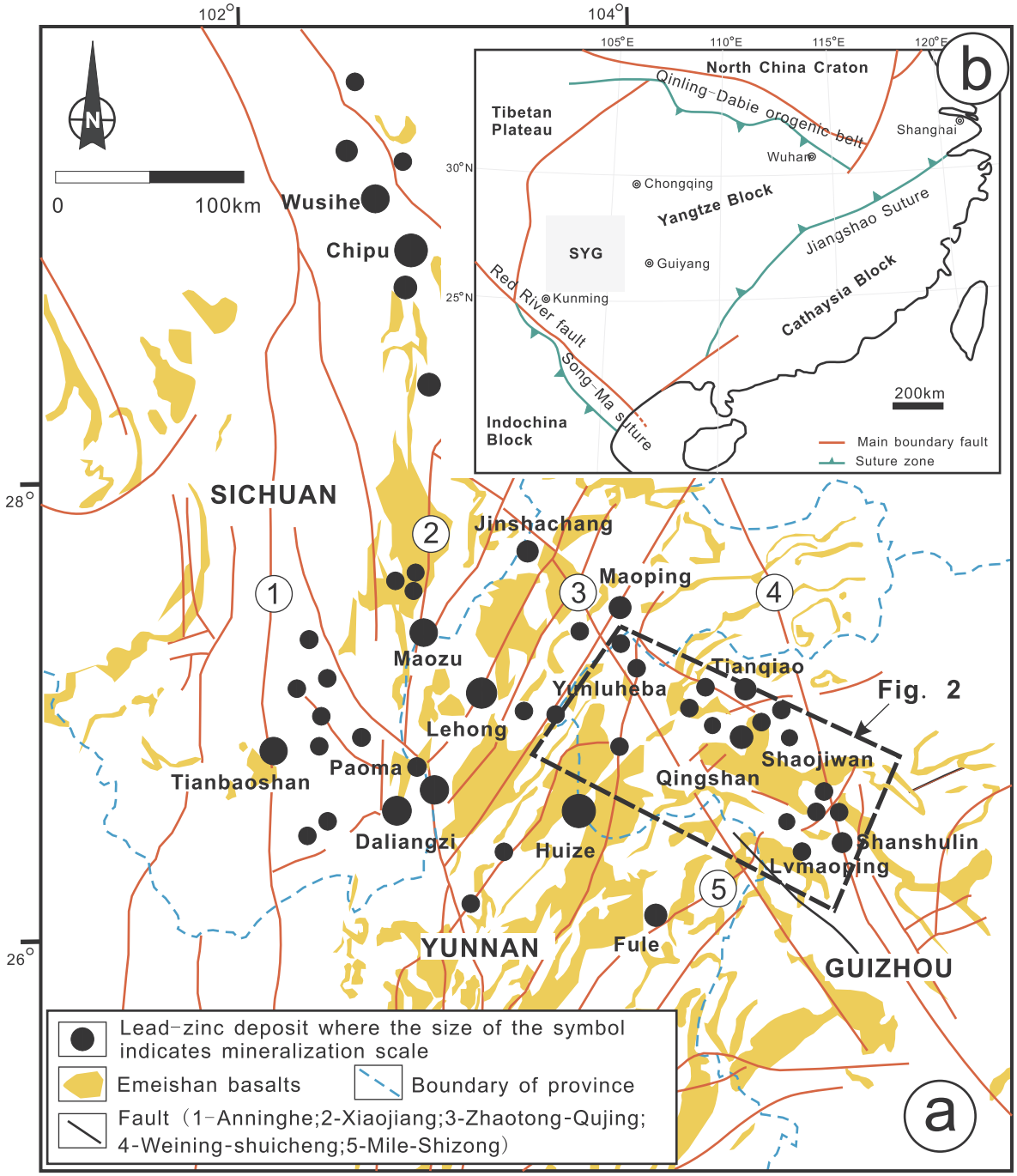

Fig. 1. (a) Regional geological map of the SYG Pb-Zn metallogenic province showing the spatial relationships among the deep faults, Emeishan flood basalts and major Pb-Zn deposits (modified from Huang et al. (2004)). The insert (b) is a tectonic map of the South China Craton showing the location of the SYG region at a larger scale.

host rocks by thermochemical sulfate reduction (Hu et al., 2017b; Kong et al., 2018; Li et al., 2006; Liu et al., 2017; Zhou et al., 2018a, 2018b). However, many of the deposits hosted by the Devonian carbonates have been found to be characterized by low $\delta^{34}S$ values (−7.8‰ to 2.7‰, Zhu et al., 2016; Zhang et al., 2016), which some have interpreted to be mantle or igneous in origin (e.g., Zhang et al., 2016). This interpretation challenges the existing genetic models for the SYG carbonate-hosted Pb-Zn deposits.

The Yunluheba Pb-Zn deposit is hosted in Devonian carbonate rocks in the eastern SYG province (Figs. 1 and 2) and has S isotopic compositions similar to those of the mantle (Zhang et al., 2016). Although no economically important Pb-Zn deposits have been discovered yet in the Yunluheba area, whether these low $\delta^{34}S$ values of the Pb-Zn deposits indicate a new type of Pb-Zn mineralization in the SYG province and provide information on their genesis is worthy of further studies, as these issues are crucial to understanding the regional metallogenesis and in guiding future explorations. Previous studies have paid expended considerable effort to determine the ore deposit geology and to evaluate the mineral potential (Deng and Yang, 2015; Jin and Huang, 2008; Liao and Deng, 2002; Yang, 2015), but knowledge of the ore sources and the mineralization age remain limited, hindering the development of an accurate genetic model.

Direct dating of hydrothermal deposits is critical for properly evaluating their relationships with notable geotectonic events;

Table 1
General characteristics of major lead-zinc deposits in the SYG area.

Deposits	Administrative affiliation	Reserves and grade	Ore-controlling structures	Orebody	Paragenetic mineralogy	Alteration	Host rocks	Ages (Ma)
Huize	Yunnan	> 5 Mt Pb + Zn, 800 t Ge; Pb + Zn > 25%	NE-trending thrust faults	Stratiform, lenticular	Galena, sphalerite, pyrite, arsenopyrite, chalcopyrite, bornite; calcite, dolomite, quartz	Dolomitization, calcification, silification, argillization	Early Carboniferous dolostone	223.5 ± 3.9, 226 ± 6.4, 196.3 ± 1.8 (sphalerite Rb-Sr)
Maoping	Yunnan	> 2 Mt, Pb + Zn > 25%	NW-trending anticline and NW-trending faults	Stratiform, lenticular, vein	Sphalerite, galena, pyrite, calcite, quartz	Dolomitization, calcification, silification, baritization	Late Devonian and Carboniferous dolostone and limestone	321.7 ± 5.8 (sphalerite Rb-Sr)
Jinshachang	Yunnan	> 1 Mt, Pb + Zn > 10%	NWW-trending anticline and NW-trending thrust fault	Strata-bound, vein	Sphalerite, galena, pyrite, calcite, quartz, fluorite, dolomite	Dolomitization, calcification, silification, baritization	Late Sinian and Early Cambrian dolostone	200.1 ± 6.2 (fluorite Sm-Nd); 206.8 ± 3.7 (sphalerite Rb-Sr)
Lehong	Yunnan	6–12% Pb + Zn	NW-trending fault	Stratiform, lenticular, vein	Sphalerite, galena, pyrite, arsenopyrite, dolomite, quartz	Baritization, dolomitization, ferritization	Late Sinian dolostone	200.9 ± 8.3 (sphalerite Rb-Sr)
Maozu	Yunnan	> 1 Mt, Pb + Zn > 12%	NE-trending thrust and anticline	Stratiform	Sphalerite, galena, calcite, dolomite, quartz, fluorite	Silification, baritization, fluoritization	Late Sinian dolostone	196 ± 13 (calcite Sm-Nd)
Tianbaoshan	Sichuan	2.6 Mt, 10–15% Pb + Zn	NW-trending thrust faults	Stratiform, lenticular, vein	Sphalerite, galena, chalcopyrite, dolomite, calcite, quartz	dolomitization, calcitization, silification	Late Sinian dolostone	> 166 (zircon U-Pb age of diabase)
Daliangzi	Sichuan	> 1 Mt, Pb + Zn > 10%	NW-trending thrust faults	Lenticular, vein, cystic	Sphalerite, galena, pyrite, arsenopyrite, chalcopyrite, tetrahedrite, quartz, calcite, dolomite	Carbonization, silification, dolomitization	Late Sinian dolostone	204.4 ± 1.2 (calcite Sm-Nd)
Chipu	Sichuan	Pb + Zn > 12%	NW-trending thrust faults	Stratiform, lenticular	Sphalerite, galena, pyrite, dolomite, calcite, quartz, bitumen	Silification, calcitization, bituminization	Late Sinian dolostone	292.0 ± 9.7, 165.7 ± 9.9 (bitumen Re-Os)
Paoma	Sichuan	> 0.2 Mt, Pb + Zn > 10%	NS-trending faults	Stratiform, lenticular	Sphalerite, galena, pyrite, fluorite, dolomite, calcite, quartz	Silification, calcitization	Late Sinian dolostone	200 ± 1 (sphalerite Rb-Sr)
Shanshulin	NW Guizhou	> 0.5 Mt, Pb + Zn > 20%	NW-trending thrust faults	Stratiform, vein	Sphalerite, galena, pyrite, dolomite, calcite	Calcitization, dolomitization	Late Carboniferous dolomitic limstone	
Shaojiwan	NW Guizhou	> 0.4 Mt, Pb + Zn > 12%	NW-trending thrust-fold	Stratiform	Sphalerite, galena, pyrite, dolomite, calcite	Calcitization, dolomitization	Early Permian and Middle Devonian limestone, dolomitic limestone and dolostone	
Qingshan	NW Guizhou	> 0.3 Mt, Pb + Zn > 15%	NW-trending thrust faults	Stratiform	Sphalerite, galena, pyrite, dolomite, calcite	Calcitization, dolomitization	Carboniferous and Permian dolomitic limestone	
Tianqiao	NW Guizhou	> 0.3 Mt, Pb + Zn > 15%	NW-trending thrust-fold	Stratiform	Sphalerite, galena, pyrite, dolomite, calcite	Calcitization, dolomitization	Carboniferous dolostone	191.9 ± 6.9 (sphalerite Rb-Sr)
Yunluheba	NW Guizhou	< 0.1Mt, Pb + Zn > 10%	NE-trending thrust fault	Stratiform Lenticular	Sphalerite, galena, pyrite, dolomite, calcite	Calcitization, dolomitization	Middle Devonian dolostone	206.2 ± 4.9 (sphalerite Rb-Sr)
MVT	worldwide	Generally medium-small scale for single deposits but can be large in an ore district	Fault and fractures, collapsed breccia, phase transition, basement uplift, bioherm	Stratiform vein	Sphalerite, galena, pyrite, calcite, dolomite, barite, quartz	Calcitization, Wall-rock dissolution, organics, silicification	Platform carbonate (mainly dolostone)	Main formation ages: Devonian to Triassic, Cretaceous to Paleogene

References: data for the Huize deposit are from Han et al. (2007) and Yin et al. (2009); the Maoping deposit from Shen et al. (2016); the Jinshachang deposit from Wu (2013), Zhang et al. (2015) and Zhou et al. (2015); the Lehong deposit from Zhang et al. (2014); the Maozu deposit from Zhou et al. (2013c); the Tianbaoshan deposit from Wang et al. (2012) and Zhou et al. (2013a); the Daliangzi deposit from Wu (2013) and Zhang et al. (2008); the Chipu deposit from Wu (2013); the Paoma deposit from Lin et al. (2010); the Shanshulin deposit from Zhou et al. (2014a); the Shaojiwan deposit from Zhou et al. (2013b); the Qingshan deposit from Zhou et al. (2013e); and the Tianqiao deposit from Zhou et al. (2013d) and Zhou et al. (2011). The MVT data are from Leach and Sangster (1993) and Leach et al. (2005).

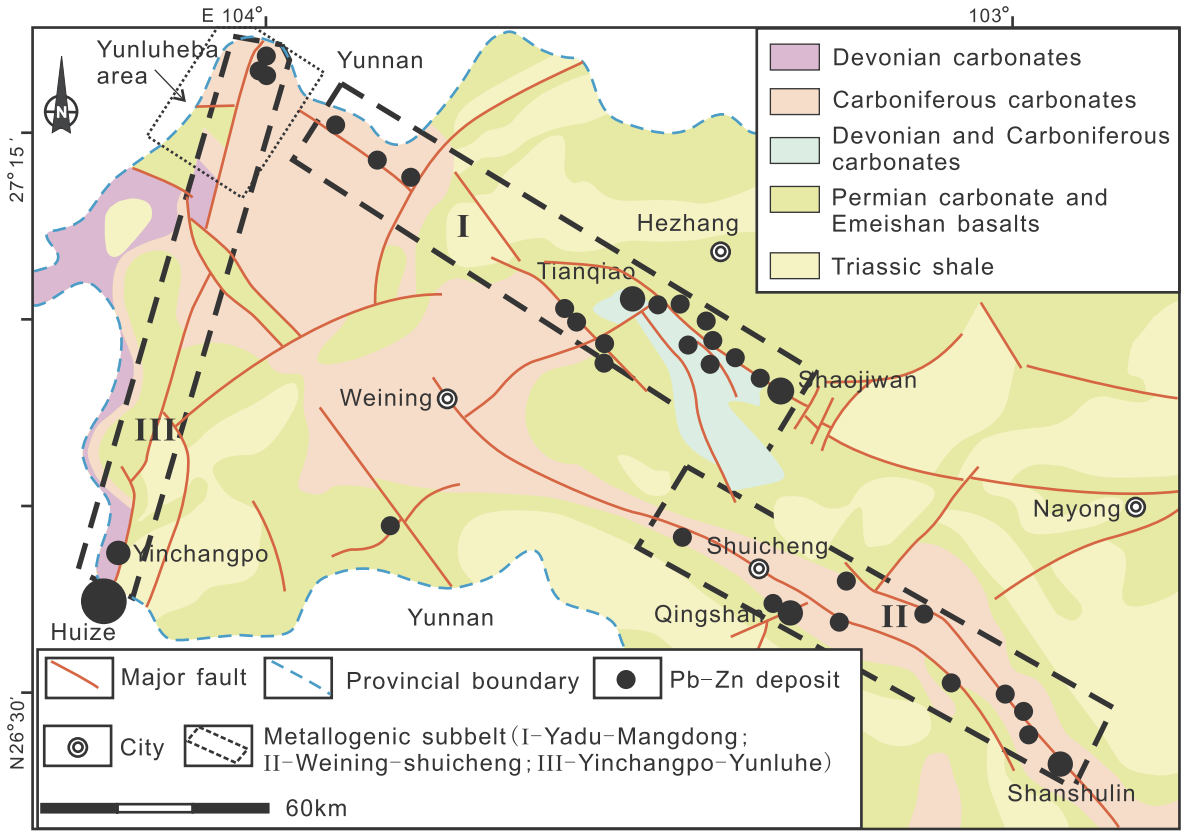

Fig. 2. Geological map of northwestern Guizhou Province showing the location of the Yunluheba Pb-Zn deposits (modified from Jin and Huang (2008)).

however, this process is challenging due to the lack of suitable minerals for traditional radioisotope dating (Li et al., 2007; Nakai et al., 1990; Sangster, 1996). The technique of sphalerite Rb-Sr dating has been greatly improved in recent decades and has become a promising tool for the direct dating of ore minerals in Zn-Pb deposits (Christensen et al., 1995; Nakai et al., 1990; Nakai et al., 1993; Nelson et al., 2002; Ostendorf et al., 2017; Schneider et al., 2007). Despite continuous concern about its reliability because of possible contamination by inclusions of carbonate, clays or volcanic ash that may impart different $^{87}Sr/^{86}Sr$ ratios (Brannon et al., 1996b), Pettke and Diamond (1995) experimentally found the Rb-Sr isotopic compositions of residual solid samples processed by crushing and cleaning to be feasible for dating a deposit. The method was applied to the MVT deposits in the Polaris and Upper Mississippi Valley areas that produced ages identical to their palaeomagnetic ages and thus were considered to represent the ore formation ages (Bradley et al., 2004). Currently, Rb-Sr sphalerite geochronology has been widely used to constrain the geodynamic settings of carbonate-hosted Pb-Zn deposits (e.g., Cao et al., 2015; Feng et al., 2017; Rosa et al., 2016; Tian et al., 2014; Xiong et al., 2018). Sulfur, lead and strontium isotopes are powerful tools that can place key constraints on the sources of ore metals and fluids as well as fluid flow pathways (e.g., Basuki et al., 2008; Leach et al., 2005; Mirnejad et al., 2011; Sebastian Staude, 2011; Tang et al., 2017); however, these elements have rarely been studied in the Yunluheba area.

To determine the genesis of the Yunluheba Pb-Zn deposit and the relationship with other deposits in the region, this study involved a comparative analysis of the Yunluheba deposit and equivalents in terms of ore deposit geology, ore formation ages, fluids and ore-forming element sources based on sphalerite Rb-Sr isotopic dating and S-Pb-Sr isotopes. The results provide new insights into the origin of the Yunluheba Pb-Zn deposit.

2. Regional geology

The Yangtze block, separated from surrounding blocks by faults and suture zones (Fig. 1), is composed of spatially limited and poorly exposed Archean and Paleoproterozoic basement assemblages that are unconformably underlain by variably deformed and metamorphosed Neoproterozoic, Paleozoic and Mesozoic igneous and sedimentary successions (Gao et al., 1999; Liu and Lin, 1999; Qiu and Gao, 2000; Wang et al., 2014). The SYG area at the southwestern margin of the Yangtze block is bounded by the Anninghe-Lvzhijiang fault in the west, the Kangding-Yiliang-Shuicheng fault in the northeast and the Mile-Shizong fault in the south. The exposed basement rocks of this region include the Dongchuan, Kangding and Kunyang Groups, which are largely composed of tightly folded but weakly metamorphosed graywackes, slates and carbonaceous to siliceous sedimentary rocks (Sun et al., 2009; Zhao et al., 2010). Paleozoic to early Mesozoic cover sequences mainly consist of shallow marine carbonates, including Cambrian black shale, sandstone and limestone interbedded with dolostone; Ordovician thick-bedded limestone and dolostone; and Devonian to Permian limestone and dolostone interlayered with minor clastic rocks (Zhou et al., 2001). Widespread Emeishan basalts unconformably lie atop the Permian carbonate rocks (Maokou Formation) in the SYG area and were derived from a mantle plume (Xu et al., 2001; Zhong et al., 2011; Hei et al., 2018). The eruption of the basalts has been dated to approximately 260 Ma (Zhou et al., 2002). The closure of the Paleo-Tethys ocean was followed by the collision of the South China plate and the Indochina block in the Early to Middle Triassic (Indosinian orogeny, 250–230 Ma; Faure et al., 2014; Qiu et al., 2017), which resulted in the formation of a series of thrust faults (Maluski et al., 2001; Xia et al., 2004; Yan et al., 2006) and foreland basins (e.g., Youjiang basins to the southeast) in the periphery of the SYG area (Jia et al., 2006; Yang et al., 2012; Yong et al., 2003).

The SYG Pb-Zn deposits are commonly hosted in Neoproterozoic to

Permian carbonate rocks in the form of stratiform, lenticular and vein orebodies controlled by thrust faults (Table 1). The ore minerals are mainly sphalerite and galena with minor pyrite, arsenopyrite, chalcopyrite and bornite, and the gangue minerals are calcite, dolomite and quartz. Wall rock alterations include dolomitization, calcification, silicification and ferritization. Faulting structures are abundant in the region and controlled the distribution of the Pb-Zn deposits (Fig. 1). In the west of the SYG region, NS-trending faults (e.g., the Xiaojiang and Anninghe faults) and their secondary structures controlled the locations of the Daliangzi, Tianbaoshan, Maozu and Chipu deposits, while in the east, the deposits were mainly influenced by NW- and NE-trending faults. The intersection sites of faults are the preferred locations for large to giant deposits. The Huize deposit, the largest Pb-Zn deposit in the SYG region, contains > 5 Mt of Pb + Zn (at grades of 25–35%, locally higher than 60%) and 800 tons of Ge (at a grade of 400 ppm; Han et al., 2007) and is associated with a NE-trending fault (the Dongchuan-Zhenxiong fault). The studied area of Yunluheba is located at the intersection of the NE-trending Yinchangpo-Yunluhe fault and the NW-trending Yiliang-Shuicheng fault (Fig. 2).

3. Geology of the Yunluheba deposit

The Yunluheba area, situated to the northwestern Weining County in NW Guizhou Province, is considered a northern extension of the NE-trending Huize Pb-Zn mineralization belt (Fig. 2; Jin et al., 2016; Zhang et al., 2016). The Pb-Zn deposits are mainly controlled by the NE-trending Yinchangpo-Yunluhe fault, which, together with the NW-trending Yadu-Mangdong and Weining-Shuicheng faults, influenced the locations of the majority of Pb-Zn deposits in NW Guizhou Province. The strata cropping out in the Yunluheba area include middle-upper Devonian, Carboniferous and lower Permian carbonate interbedded with a lesser amount of clastic rocks. The orebodies are mainly hosted in coarsely crystallized dolostone and dolomitic limestone of the Middle Devonian Wangchengpo Formation and Carboniferous Dabu and Huanglong Formations. The major ore-controlling structure, the Yinchangpo-Yunluhe fault, is a sinistral transpressional high-angle thrust fault with a dip direction of 100–150° and a dip angle of 60–70°. Fault intersections, the dipping ends of anticlines and inversions are the preferred structures for ore emplacement.

Dozens of small-scale Pb-Zn deposits, including Haoxing, Fuqiang, Shunda, Tangjiapingzi and Shizidong, have been discovered in the Devonian dolostone and are spatially restricted to fault zones as well as derivative branching faults and interlaminar fractures (Fig. 3). Orebodies are present as stratiform and lens-like shapes and run parallel to the bedding of the wall rocks. These deposits commonly display clear vertical zoning from oxidized ore at the top to mixed ore in the middle to primary sulfides at the bottom. The thickness of the oxidized ore varies from a few meters to more than hundreds of meters, and currently, only a few deposits (e.g., Haoxing) have been found with a considerable reserve of sulfides. A wide range of alteration types, including dolomitization, ferritization, calcitization and silicification, are observed in the wall rocks. The primary sulfide minerals include galena, sphalerite and pyrite, and the gangue minerals are dolomite, calcite and quartz. Ores are mainly present in massive, spotted, veined, brecciated and disseminated textures and in certain cases in allotriomorphic granular, metasomatic relict and crush textures (Fig. 4).

Based on the relationships of crosscutting and paragenetic assemblages, the representative of the Haoxing deposit underwent synsedimentation, hydrothermal mineralization and supergene oxidation (Fig. 5). The *syn*-sedimentation stage is characterized by fine-grained disseminated euhedral pyrite (Fig. 4E and G) accompanied by minor dolomite and calcite. This stage was a major stage for pyrite growth, which recrystallized later in the hydrothermal stage. The hydrothermal mineralization is characterized by an early pyrite-sphalerite-quartz stage and a late pyrite-sphalerite-galena-dolomite-calcite stage (Fig. 4A–D). Sphalerite mainly formed in the early stage and commonly exhibits coarse-grained vein and massive textures (Fig. 4A and F). The sphalerite was fractured and filled with late-stage galena and calcite (Fig. 4H) and was occasionally replaced or entrapped by galena. Sphalerite are compositionally homogeneous, and no special textures (e.g., core-mantle and zoning) have been found (Fig. 4I). Galena is commonly observed to have been replaced by cerussite. Supergene minerals, including limonite, smithsonite, hematite and cerussite, are present as gossan.

4. Samples and analytical methods

Sphalerite samples used for isotopic analysis in this study were collected from the Haoxing and Fuqiang deposits (Tables 2–4). Those for Rb-Sr dating are all from the Haoxing deposit. The samples were crushed to a size of 60–80 mesh for handpicking under a binocular microscope. The estimated purity of the separates exceeded 99%. The separates were then ground to less than 200 mesh using an agate mortar before dissolution.

For the Rb-Sr isotope analysis, sample aliquots were cleaned with ultrapure water in an ultrasonic bath three times to remove salts from broken fluid inclusions. Each sample was spiked with mixed isotopic tracers and dissolved with ultrapure 6 mol/L HCl and HNO_3 in a sealed Teflon cup at 200 °C in an oven. The samples were dried on a hot plate and then redissolved with ultrapure 6 mol/L HNO_3. These samples were then transferred to cation exchange resin columns for the separation and purification of Rb and Sr. For a detailed description of the procedure, refer to Wang et al. (2007) and Wang et al. (1988). The isotopic ratios were measured on a British VG354 multicollector mass spectrometer at the Center of Modern Analysis, University of Nanjing, China. The total procedural blanks were less than 5×10^{-9} g for Rb and Sr. The international standard NBS-987 was analyzed to correct for the instrumental fractionation of the Sr isotopes. The measured $^{87}Sr/^{86}Sr$ value of the standard was 0.710233 ± 6, which is consistent with the recommended value (0.71023 ± 5; Cao et al., 2015). The errors (σ) were 1% and 0.005% for the $^{87}Rb/^{86}Sr$ and $^{87}Sr/^{86}Sr$ ratios, respectively. The Rb-Sr isochron regression and age calculations were performed using Isoplot/Ex version 3.22 software (Ludwig, 2005).

The sulfur isotope analyses were conducted using a Thermo Fisher MAT-253 gas-source mass spectrometer at the State Key Laboratory of Ore Deposit Geochemistry, Institute of Geochemistry, Chinese Academy of Sciences (IGCAS). Aliquots of the samples were oxidized to SO_2 gas by Cu_2O in a muffle furnace under high-temperature (1000 °C) vacuum conditions; then, the $\delta^{34}S$ values of the resulting SO_2 gas were measured with analytical uncertainties of 0.2‰ (2σ). The sulfur isotope compositions are reported relative to the Vienna Canyon Diablo Troilite (V-CDT) standard.

Lead isotope analysis was carried out on a Finnigan MAT 261 Thermo Ionized Mass Spectrometer at the Wuhan Center of Geological Survey (WCGS), China Geological Survey. All samples were cleaned with ultrapure water before dissolution by ultrapure HCl and HF. The separation and purification of Pb were performed with HBr and anion exchange resin (AG-1 × 8 200–400 mesh) columns. The internal precision of Pb isotope ratios was better than 0.1%, and the replicate analyses were consistent within the error. The measured $^{207}Pb/^{206}Pb$ value of the standard NBS-981 was 0.91454 ± 6, which is consistent with the reference value (0.91464 ± 33). For more details, refer to Lu et al. (2016).

5. Results

The concentrations and isotopic compositions of Rb and Sr in sphalerite are shown in Table 2. Seven sphalerite separates exhibited Rb and Sr concentrations ranging from 0.06 to 0.65 ppm and from 0.23 to 2.55 ppm, respectively. The $^{87}Rb/^{86}Sr$ ratios varied from 0.15 to 3.46, and the $^{87}Sr/^{86}Sr$ ratios varied from 0.71086 to 0.72045. The samples showed a linear correlation in the $^{87}Rb/^{86}Sr$ vs. $^{87}Sr/^{86}Sr$ space

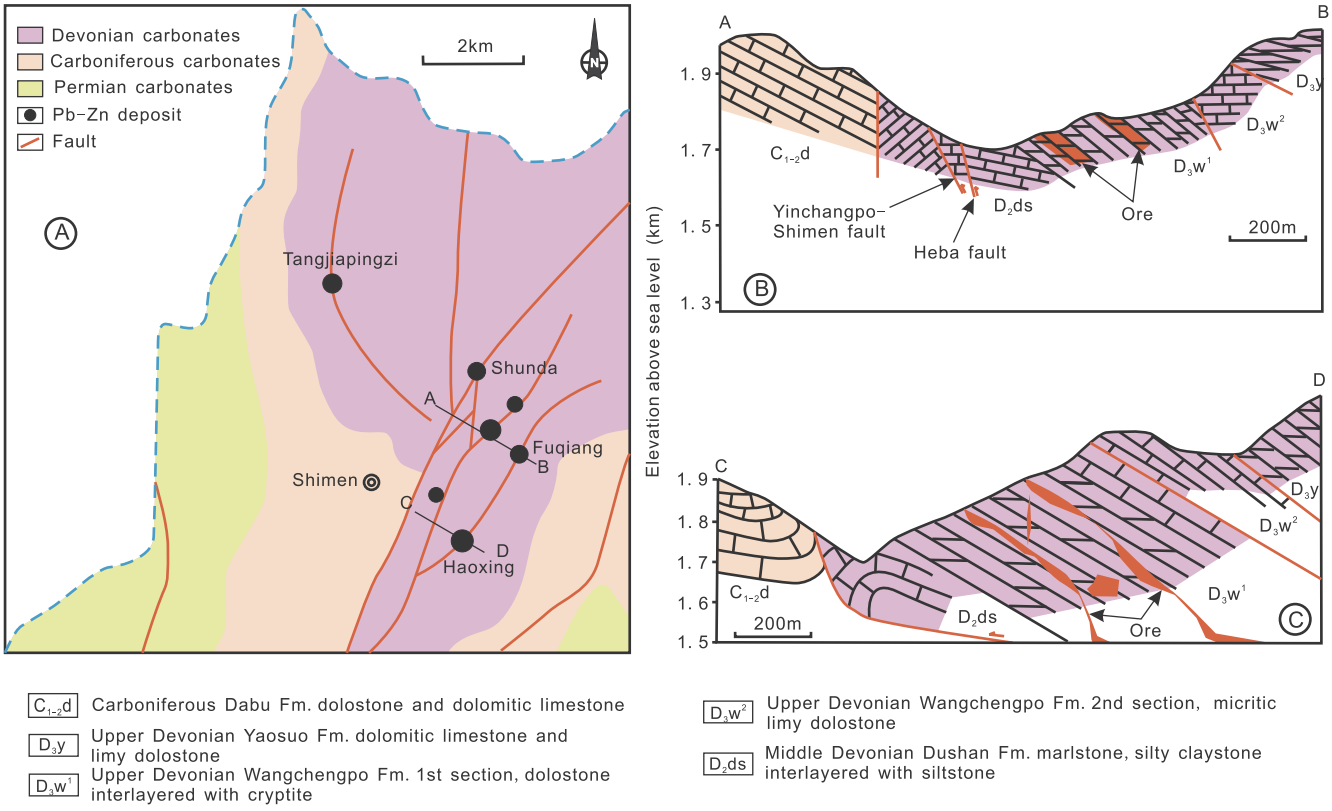

Fig. 3. Geological map of the Yunluheba area showing the distribution of major Pb-Zn deposits and their relationship with major structures (A) and a cross section through the Fuqiang (B) and Haoxing deposits (C).

(Fig. 6A), corresponding to an isochron age of 206.2 ± 4.9 Ma with an MSWD of 1.9 (Model 3 solution; Ludwig, 2005).

Except for an outlier ($\delta^{34}S = -18.1‰$) measured from pyrite (Table 3), the sulfur isotope compositions of sphalerite and galena are homogeneous with $\delta^{34}S$ values ranging from −2.0 to 2.9‰ and peaking at 0‰ in the Yunluheba deposit (Fig. 7A). The S isotopic features of the Yunluheba deposit are remarkably different from those of most of the SYG Pb-Zn deposits which show $\delta^{34}S$ values in a range of 8‰ to 20‰ (Fig. 7B).

The $^{206}Pb/^{204}Pb$, $^{207}Pb/^{204}Pb$ and $^{208}Pb/^{204}Pb$ ratios range from 18.196 to 18.658, 15.645 to 15.897, and 38.415 to 39.465, respectively. It is notable that the Pb isotope data plot above the orogenic evolution curve in a nearly linear array in $^{207}Pb/^{204}Pb$ vs. $^{206}Pb/^{204}Pb$ space (Fig. 8). Moreover, the Pb isotopic compositions show excellent consistency with the age-corrected Pb isotopic compositions of the Devonian to Permian carbonate rocks. The Yunluheba deposit has Pb isotopic compositions comparable to those of the Huize, Yinchangpo, Shanshulin Shaojiwan and Qingshan deposits, which form linear arrays extending overall within the range of the Devonian to Permian carbonate rocks. The Pb isotopic compositions of the Tianqiao deposit are relatively homogenous and fall within the Pb isotopic range of the basement rocks.

6. Discussion

6.1. Timing of the Pb-Zn mineralization in the Yunluheba deposit

Despite the possibility of exotic Sr involvement, the process of crushing followed by cleaning for sphalerite separates can greatly diminish the interference of fluid inclusions of either primary or secondary origin; thus, the date obtained from the solid residue more likely represents the ore formation age (Liu et al., 1998; Pettke and Diamond, 1995). Given that the $^{87}Sr/^{86}Sr$ and 1/Sr ratios of the sphalerite are not linearly correlated (Fig. 6B), this indicates that the isochron (Fig. 6A) is not a pseudo-isochron of two-component mixing and thus should reflect the timing of the Pb-Zn mineralization (Nakai et al., 1993; Rosa et al., 2016; Schneider et al., 2003; Xiong et al., 2018). Geologically, the Yunluheba Pb-Zn deposits are spatially controlled by the NE-trending Yinchangpo-Yunluhe thrust fault, which implies that the Pb-Zn mineralization should have postdated the thrusting; however, no data are available to constrain the timing of the overthrusting movement. The youngest strata involved in the foot wall are the Permian Feixianguan Formation that was deposited at 252–247 Ma (Liao and Deng, 2002), which may provide an upper age limit for the Yunluheba deposit. Thus, the Pb-Zn ore formation likely took place after the deposition of the Feixianguan Formation. The sphalerite Rb-Sr dating result (206.2 ± 4.9 Ma) for the Yunluheba deposit agrees with this scenario. The Yunluheba Rb-Sr age is approximately identical within reasonable uncertainty to the ages of many other SYG deposits (Table 1 and Fig. 9; Lin et al., 2010; Zhang et al., 2015; Zhang et al., 2014; Zhou et al., 2013c; Zhou et al., 2013d; Zhou et al., 2015). For ages acquired by various isotopic systematics, although many are from Rb-Sr isotopic dating, the coincidence provides added credibility to the Yunluheba Rb-Sr date and suggests that the Rb-Sr geochronology is applicable to most SYG Pb-Zn deposits. Therefore, we conclude that the Yunluheba Pb-Zn deposit was formed synchronously with most of the SYG Pb-Zn deposits by a regional hydrothermal event during the late Indosinian orogeny (Hu et al., 2017b; Zhang et al., 2015; Zhou et al., 2015).

6.2. Ore sources

The Pb isotopic compositions of sulfides in the Yunluheba deposit vary considerably and form a linear trend in $^{207}Pb/^{204}Pb$-$^{206}Pb/^{204}Pb$ space (Fig. 8). Three possible scenarios may result in a linear array: analytical errors, a secondary isochron and binary mixing (Franklin, 1983). Leach et al. (2005) documented mass discrimination errors

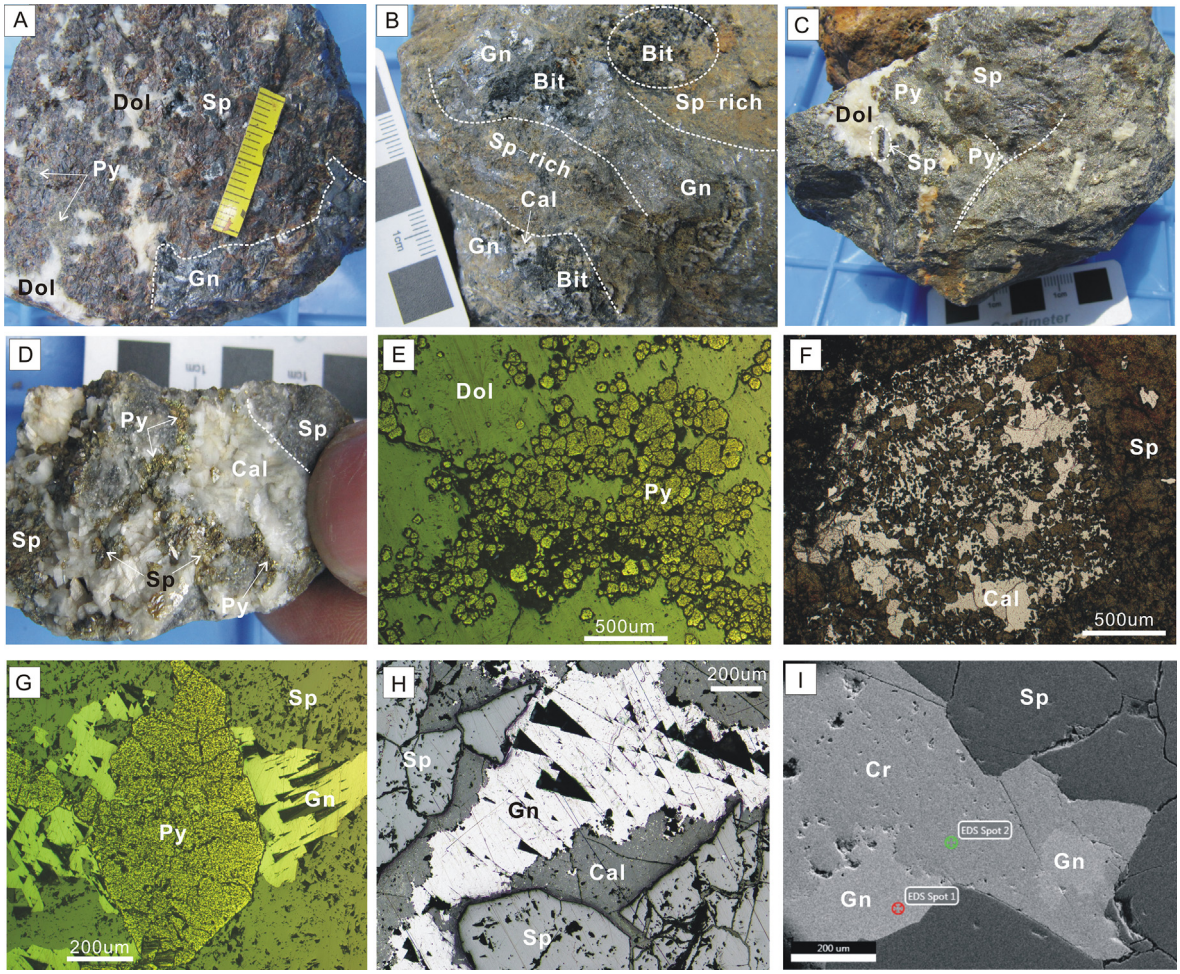

Fig. 4. Mineralization features of ore specimens and photomicrographs. A. Early-stage massive sphalerite invaded by late-stage dolomite and galena. B. Late-stage coarse-grained galena intergrown with calcite and bitumen, which cuts the early-stage sphalerite ore. C. Synsedimentary pyrite was intruded by early-stage brown sphalerite, which was subsequently cut or included by late-stage dolomite. D. Late-stage vein comprising calcite, pyrite and minor yellowish sphalerite, cutting early-stage sphalerite ore. E. Early-stage hydrothermal pyrite filling the fractures and cavities of dolostone (reflected light). F. Early-stage massive sphalerite replacing limestone (transmitted light). G. Early-stage massive sphalerite ore containing relics of earlier fractured pyrite altered by galena (reflected light). H. Late-stage calcite and galena filling the fractures of early-stage sphalerite. I. Compositionally homogeneous sphalerite is intruded by a galena vein, which has been replaced by cerussite (SEM image). Abbreviations: Cal-calcite, Cr-cerussite, Dol-dolomite, Gn-galena, Py-pyrite, and Sp-sphalerite.

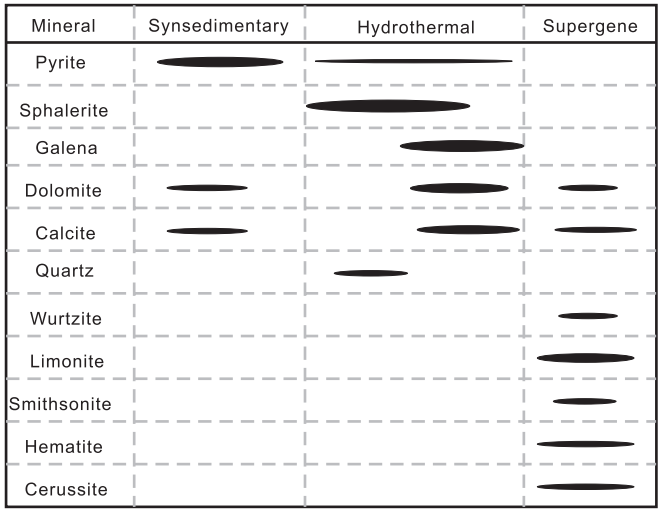

Fig. 5. Paragenetic sequence of major minerals in the Yunluheba deposit. The heights of the filled ellipses indicate the abundance of minerals.

caused by slight variations in filament temperatures and sample loads that produce arrays with a constant slope of ~1.4; clearly, this process does not likely apply to the Yunluheba deposit. The Pb isotope data (excluding an analysis that deviates from the trend) define a straight line (with a slope of 0.8171) that yields a two-stage model age of 228 Ma at the intersection with the Pb growth curve of the Stacey-Kramers model (Faure and Mensing, 2005). This date may represent the time at which the Pb was withdrawn from the second Stacey-Kramers reservoir; subsequently, the Pb was mixed with radiogenic Pb and deposited in the sulfides. Alternatively, the trend was caused by the mixing of two isotopically distinct sources (high μ and low μ sources, where μ = Th/U). The majority of Pb isotopic analyses plot above the crustal Pb evolution curve, indicating that the ore Pb has a predominantly crustal source (Zartman and Doe, 1981). Moreover, the Pb isotopic compositions are comparable to those of age-corrected Devonian to Permian carbonate rocks, indicating that the Pb was largely derived from the carbonates. Carbonates are typically enriched in U but depleted in Th (Ostendorf et al., 2017; Rosa et al., 2016), thereby potentially accounting for the low μ source. The basement metamorphic rocks, generally characterized by U loss (high μ) due to high-grade metamorphism (Dostal and Capedri, 1978; Downes et al., 2001), lie at the bottom of the data trend. Therefore, the basement rocks probably represent the other Pb source but contributed only a small amount. This

Table 2
Sphalerite Rb-Sr isotopic compositions of the Haoxing Pb-Zn deposit.

Sample	Description	Rb/ppm	Sr/ppm	$^{87}Rb/^{86}Sr$	$^{87}Sr/^{86}Sr$	$^{87}Sr/^{86}Sr_{200Ma}$
HX14-20-1	Stage-1 massive sphalerite	0.08	1.57	0.15 ± 0.01	0.71086 ± 5	0.7104
HX14-23	Stage-1 vein sphalerite	0.18	2.55	0.21 ± 0.01	0.71089 ± 5	0.7103
HX14-15C	Stage-1 tawny sphalerite	0.65	0.55	3.46 ± 0.01	0.72045 ± 5	0.7107
HX14-20-2	Stage-1 brown sphalerite	0.73	1.84	1.83 ± 0.01	0.71573 ± 5	0.7106
HX14-21	Stage-1 massive brown sphalerite	0.06	0.23	0.79 ± 0.01	0.71262 ± 5	0.7104
HX14-16A	Stage-1 massive brown sphalerite	0.45	2.37	0.56 ± 0.01	0.71206 ± 5	0.7105
HX14-19	Stage-1 massive brown sphalerite	0.31	2.32	0.39 ± 0.01	0.71136 ± 5	0.7103

Note: $(^{87}Sr/^{86}Sr)_t = {}^{87}Sr/^{86}Sr - {}^{87}Rb/^{86}Sr * (e^{\lambda t} - 1)$, $\lambda_{Rb} = 1.41 * 10^{-11}t^{-1}$, t = 200 Ma.

Table 3
Sulfur isotopic compositions of sulfides from the Yunluheba Pb-Zn deposits.

Sample	Deposit	Mineral	$\delta^{34}S_{CDT}$	Reference
HX14-20-1	Haoxing	Sphalerite	1.7	This study
HX14-23	Haoxing	Sphalerite	2.0	
HX14-15C	Haoxing	Sphalerite	−0.2	
HX14-20-2	Haoxing	Sphalerite	1.3	
HX14-21	Haoxing	Sphalerite	2.9	
HX14-16A	Haoxing	Sphalerite	1.1	
HX14-19	Haoxing	Sphalerite	0.9	
HX14-18	Haoxing	Sphalerite	1.5	
FQ14-15D	Fuqiang	Sphalerite	−1.6	
FQ14-16B	Fuqiang	Sphalerite	−0.9	
467-6	Haoxing	Galena	2.7	Zhang et al., 2016
467-6	Haoxing	Sphalerite	−0.1	
467-3	Haoxing	Galena	−1.5	
467-9	Haoxing	Galena	−1.3	
467-9	Haoxing	Sphalerite	0.5	
467-2a	Haoxing	Galena	−2.0	
467-2a	Haoxing	Sphalerite	0.2	
467-7	Haoxing	Pyrite	−18.1	
467-7	Haoxing	Galena	0.9	
467-7	Haoxing	Sphalerite	−0.3	

interpretation also applies to the Pb isotopic variations in the Huize, Yinchangpo, Qingshan and Shanshulin deposits, but there are differences in the proportions of the contained basement Pb. The Pb of the Tianqiao deposit may have been derived from a homogenized source of basement Pb, in consideration of its limited Pb isotopic variations which are largely characteristic of the basement rocks (Fig. 8). The Emeishan basalts contributed no significant amount of Pb to any of the deposits.

The initial $^{87}Sr/^{86}Sr$ values of the Yunluheba ore fluid range from 0.7103 to 0.7107, slightly lower than the values (0.7107–0.7132) of the Shanshulin, Shaojiwan, Tianqiao and Jinshachang deposits but very different from those for the Huize deposit (Fig. 10). The Yunluheba, Shanshulin, Tianqiao and Jinshachang deposits are generally characterized by low $^{87}Sr/^{86}Sr$ ratios that are more similar to the range (0.7073–0.7111) of the Devonian to Permian carbonate rocks, indicating that the Sr was mainly derived from the marine carbonates. No significant amount of Sr was extracted from either the basement rocks or the Emeishan basalts. The Yunluheba, Jinshachang and Tianqiao deposits have very limited variations in initial Sr isotopic values in their sphalerite residues, implying that the Sr of the ore fluids is isotopically homogeneous and that the Sr could have been extracted from a specific source for each deposit, which is likely an important cause of success in sphalerite Rb-Sr dating in the deposits. The Shanshulin and Shaojiwan deposits are characteristic of relatively wide ranges of initial Sr ratios, which indicates that the Sr is likely a mixture of various marine sources. The Huize deposit, characterized by considerably varied and much higher $^{87}Sr/^{86}Sr$ values, likely includes a large amount of Sr from the basement rocks.

Previous studies have concluded that the sulfur associated with the formation of the Yunluhede deposits is mantle in origin because the $\delta^{34}S$ values of sulfides are mainly concentrated from −1.5‰ to 2.7‰ (Zhang et al., 2016). In this study, we expanded the quantity of samples

Table 4
Lead isotopic compositions of sulfides from the Yunluheba Pb-Zn deposits.

Sample	Deposit	Mineral	$^{206}Pb/^{204}Pb$		$^{207}Pb/^{204}Pb$		$^{208}Pb/^{204}Pb$		Reference
			Ratio	2σ	Ratio	2σ	Ratio	2σ	
HX14-20-1	Haoxing	Sphalerite	18.553	0.003	15.775	0.003	39.055	0.004	This study
HX14-23	Haoxing	Sphalerite	18.658	0.005	15.897	0.005	39.465	0.011	
HX14-15C	Haoxing	Sphalerite	18.557	0.004	15.767	0.005	39.050	0.009	
HX14-20-2	Haoxing	Sphalerite	18.529	0.003	15.746	0.003	38.957	0.003	
HX14-21	Haoxing	Sphalerite	18.541	0.004	15.753	0.004	38.986	0.008	
HX14-16A	Haoxing	Sphalerite	18.570	0.005	15.788	0.004	39.085	0.009	
HX14-19	Haoxing	Sphalerite	18.556	0.003	15.770	0.002	39.051	0.005	
HX14-18	Haoxing	Sphalerite	18.537	0.005	15.796	0.005	39.104	0.007	
FQ14-15D	Fuqiang	Sphalerite	18.584	0.007	15.810	0.006	39.191	0.013	
FQ14-16B	Fuqiang	Sphalerite	18.537	0.003	15.770	0.004	39.089	0.006	
467-6	Haoxing	Galena	18.385	0.003	15.665	0.004	38.713	0.007	Zhang et al., 2016
467-6	Haoxing	Sphalerite	18.41	0.003	15.666	0.003	38.757	0.005	
467-3	Haoxing	Galena	18.196	0.003	15.645	0.003	38.415	0.007	
HX14-25d	Haoxing	Pyrite	18.414	0.003	15.67	0.003	38.769	0.006	
FQ14-16d	Fuqiang	Galena	18.431	0.004	15.676	0.005	38.804	0.009	
FQ14-53b	Fuqiang	Pyrite	18.439	0.002	15.676	0.003	38.838	0.007	
FQ14-55	Fuqiang	Sphalerite	18.439	0.003	15.686	0.003	38.870	0.003	
SD14-9a	Shunda	Galena	18.459	0.006	15.703	0.002	38.906	0.008	
SD14-10a	Shunda	Galena	18.441	0.004	15.692	0.004	38.876	0.008	
SD14-11a	Shunda	Pyrite	18.496	0.004	15.723	0.004	38.938	0.008	
SZD13-30	Shizidong	Pyrite	18.513	0.002	15.721	0.002	39.018	0.005	
SZD14-43d	Shizidong	Pyrite	18.525	0.003	15.731	0.003	39.058	0.005	

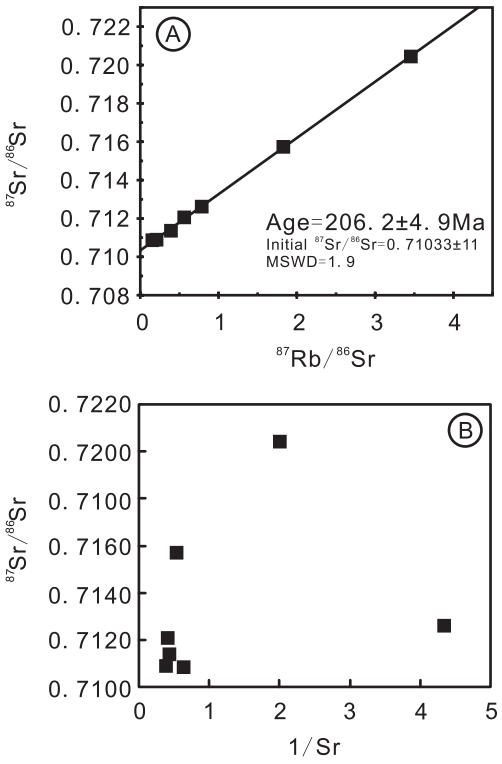

Fig. 6. Sphalerite Rb-Sr isochron (A) and $^{87}Sr/^{86}Sr$ vs. 1/Sr diagrams (B).

for sulfur isotope analysis and acquired compositions (−2.0‰ to 2.9‰) similar to those in previous research. With consideration of the absence of paragenetic sulfates, the $\delta^{34}S$ values of sulfides could represent the total sulfur isotopic composition ($\delta^{34}\Sigma S$) of the fluid from which the sulfides precipitated and thus can be used to directly trace the sulfur sources (Ohmoto and Rye, 1979). Therefore, two possibilities can be invoked to account for the sulfur source, i.e., a single mantle source or a mixed source involving sulfur from biogenic and seawater sources (Machel, 2001; Ohmoto and Rye, 1979). Our dating result suggests that the Yunluheba deposit, along with most of the SYG carbonate-hosted Pb-Zn deposits, formed at approximately 200 Ma in response to a regional hydrothermal event likely triggered by the late Indosinian orogeny (Fig. 9). Moreover, the Pb and Sr isotope compositions of the Yunluheba deposit are clearly similar to those of the host rocks (as well as to some degree those of the basement rocks), which acted as sources of ore material, as observed in many other deposits (Figs. 8 and 10). Under such circumstances, it is difficult to understand why the Yunluheba deposit obtained sulfur from only the mantle, while others did not, particularly when no concurrent magmatism has, as yet, been found in the studied area. Whether a hidden Indosinian magma exists at depth cannot be determined at present, but there are a few lines of evidence suggesting Indosinian magmatism (235–204 Ma) that did take place in certain other locations in the SYG province, such as western Sichuan (Liu et al., 2004; Wang et al., 2012; Xia et al., 2004). In the SYG province, the main exposure of magmatism is the Emeishan basalts that formed at 262–256 Ma (Zhou et al., 2002), clearly predating the Pb-Zn mineralization, and the only other magmatic rocks are postore diabase dikes. Although some studies insist on a genetic link between the Emeishan basalts and the Pb-Zn deposits either in supply of ore materials or energy transfer (Huang et al., 2004; Wang et al., 2018; Xu et al., 2014; Zhou et al., 2018b), such relationships appear unconvincing based on the evidence currently available (Kong et al., 2018).

Alternatively, a two-component mixing model of sulfur from biogenic sources and stratabound thermochemically reduced sulfate seems more applicable for the interpretation of the sulfur isotopic variation in the Yunluheba deposit. In many of the SYG Pb-Zn deposits, an episode of pre-ore pyrite formation characterized by very negative $\delta^{34}S$ values and microbially relevant ore textures (e.g., colloform, framboidal, and dendritic) have been recognized; these textures are commonly considered to be products of bacterial sulfate reduction (BSR) from pore waters during preore synsedimentation or diagenesis (Wang, 1991, 1992; Wu, 2013; Yang et al., 2018). This type of pyrite was observed in the Yunluheba deposit, and the pyrite has $\delta^{34}S$ values of −18.1‰ (Zhang et al., 2016) and shows clear signatures of dissolution and alteration by later hydrothermal fluids (Fig. 4C and G). Therefore, pyrite could have been a favorable source of low $\delta^{34}S$ values. In the Yunluheba area, as well as in the wider SYG province, the universally present evaporates, such as barite, in the ore-hosting carbonate rocks show $\delta^{34}S$ values ranging from 21.8‰ to 35.4‰ (Liu and Lin, 1999; Zhang et al., 2016; Zhou et al., 2015). Considering the fluid inclusion homogenization temperatures documented for the Yunluheba deposit (164–228 °C, unpublished data from Guizhou Geological Bureau), thermochemical sulfate reduction (TSR) is a likely mechanism for the formation of reduced sulfur, consistent with the case in most of the SYG Pb-Zn deposits (Kong et al., 2018; Luo et al., 2019; Zhou et al., 2018b; Zhou et al., 2018c; Zhu et al., 2018), which yields a fractionation of 15‰ at 150 °C and 10‰ at 200 °C between reactant sulfate and product H_2S (Kiyosu, 1980; Machel, 2001). Thus, the TSR-induced $\delta^{34}S$ values of sulfides might range from 7‰ to 25‰, which exactly overlap the majority of $\delta^{34}S$ data for most of the SYG deposits (Fig. 7B). Zhang et al. (2016) reported a $\delta^{34}S$ value of 21.8‰ measured from sedimentary barite in Devonian carbonates in the Yunluheba district, which are expected to produce a variation in $\delta^{34}S$ values from 7‰ to 12‰ for H_2S via the TSR mechanism at 150–200 °C. Assuming that the average $\delta^{34}S$ value of the biogenic source from altered synsedimentary pyrite is −18‰, the addition of TSR-induced sulfur with a fraction of 0.2–0.7 of the total sulfur may result in a range of $\delta^{34}S$ values in the hydrothermal fluid that is similar to that of the Yunluheba deposit (−2‰ to 2.9‰). A similar mechanism has also been proposed to interpret the $\delta^{34}S$ variation (−2‰ to 8.1‰) of sulfides in the Tianbaoshan and Daliangzi deposits (Wang, 1991, 1992).

As shown in Table 1, the Yunluheba Pb-Zn deposits have many features in common with other SYG carbonate-hosted Pb-Zn deposits. Thus, the question arises as to why the Yunluheba deposit have distinct S isotopes from the other deposits. Zhu et al. (2016) considered that the variations in S isotopic compositions of sulfides from SYG Pb-Zn deposits are mainly related to different-aged carbonate host rocks and that the capability of those host rocks to contribute reduced S (e.g., H_2S) is crucial to the formation of the ore deposits. Some Pb-Zn deposits hosted by Devonian strata feature low $\delta^{34}S$ values (Zhang et al., 2016; Zhou et al., 2014b; Zhu et al., 2016), which may largely be attributable to the availability of reduced S in the host rocks. As noted above, the signature of low $\delta^{34}S$ values for Devonian strata-hosted deposits was dominated by the biogenic S from alteration of synsedimentary pyrite in the strata. Other deposits hosted by rocks other than the Devonian rocks characterize high $\delta^{34}S$ values of sulfides likely due to the shortage of biogenic S supply in host rocks. Because carbonate host rocks of different ages have evaporates with varying $\delta^{34}S$ values (Zhou et al., 2014b), this mainly resulted in the variations of TSR-induced $\delta^{34}S$ values of sulfides among deposits; additionally, the change in temperature for TSR reactions might have also affected the S isotopic compositions of sulfides in the deposits.

6.3. Ore-forming mechanism

Many previous studies suggest that the SYG carbonate-hosted Pb-Zn deposits are of MVT origin based on consideration of a range of similarities in host rock, tectonic setting and ore fluids (Hu et al., 2017b; Zaw et al., 2007; Zhang et al., 2015; Zheng and Wang, 1991; Zhou et al., 2001). Nonetheless, some deposits, such as Daliangzi and Huize, are thought to have a genetic connection with magmatism based on

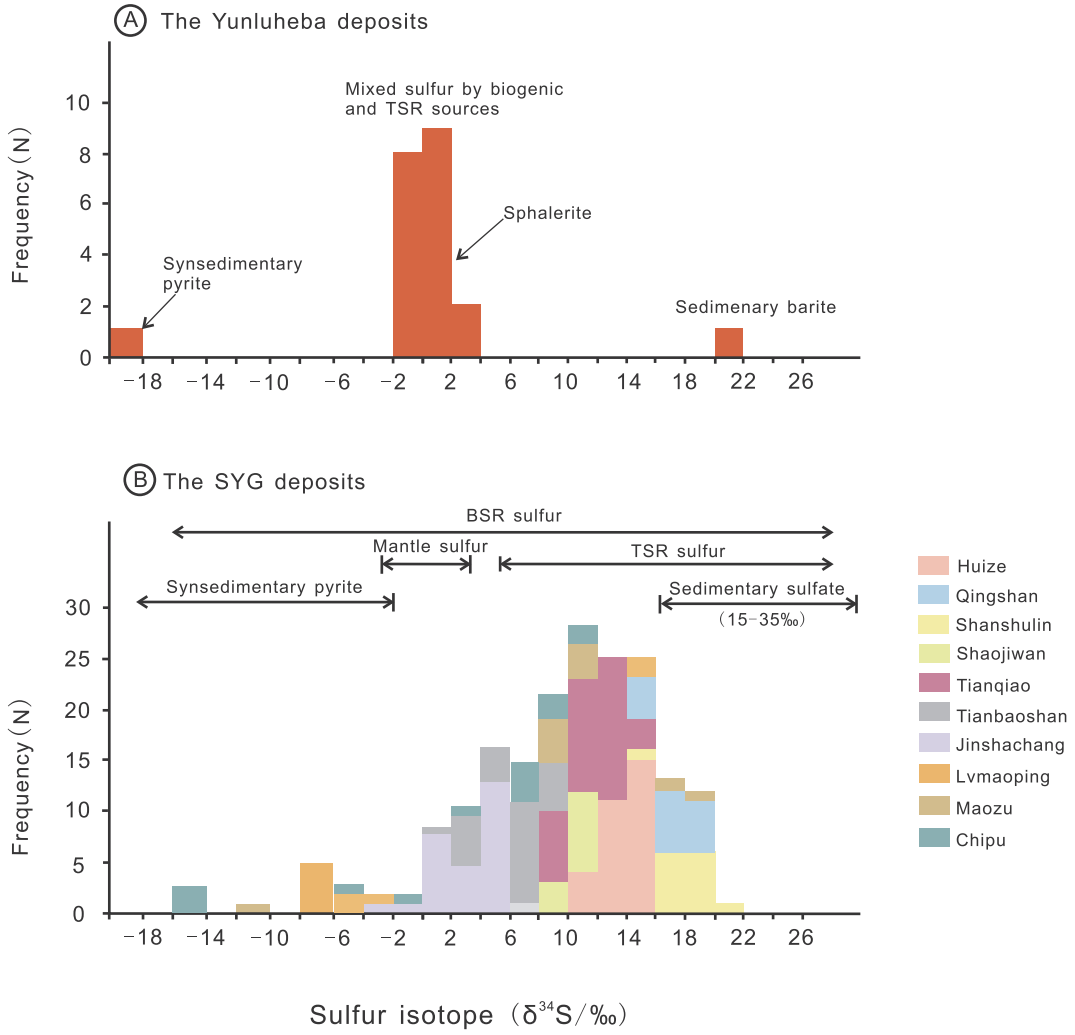

Fig. 7. Histograms of the sulfur isotopic compositions of sulfides from the Yunluheba deposit and regional analogs. The $\delta^{34}S$ data for the Huize, Shanshulin and Tianbaoshan deposits are from Liang (2017); those for the Qingshan deposit are from Zhang et al. (1999) and Zhou et al. (2013e); those for the Shaojiwan deposit are from Zhou et al. (2013b); those for the Tianqiao deposit are from Zhou et al. (2013d); those for the Jinshachang deposit are from Bai et al. (2013) and Zhou et al. (2015); those for the Lvmaoping deposit are from Zhu et al. (2016); those for the Maozu deposit are from Zhang et al. (2008); and those for the Chipu deposit are from Wu (2013). The $\delta^{34}S$ data for sedimentary sulfates are from Kong et al. (2018), Liu and Lin (1999), Zhang et al. (2016) and Zhou et al. (2015). The ranges of S isotopic compositions of bacterial sulfate reduction (BSR) and thermochemical sulfate reduction (TSR) are delineated according to Warren (1999). The sulfur isotopic range of mantle sulfur was delineated by Chaussidon et al. (1989) and Ohmoto (1986).

noble gas isotopic studies (Wang et al., 2018). By comparison, the Yunluheba deposit shares a series of characteristics, such as fault-controlled ore distributions, platform carbonate host rock, simple ore mineral compositions and stratiform or lenticular ore bodies, which, in addition to being prevalent in other SYG deposits, are also typical of MVT deposits (Table 1). The C-O isotope compositions ($\delta^{13}C_{PDB}$ = 0.3‰ to −10.1‰ and $\delta^{18}O_{SMOW}$ = 20.2‰ to 23.6‰) of the calcite and dolomite associated with the Yunluheba Pb-Zn mineralization suggest that the carbon was derived from a combination of dissolution of marine carbonates and organic matter dehydroxylation (Jin et al., 2016). Moreover, the fluid inclusions in the Yunluheba deposit have homogenization temperatures that range from 164 to 228 °C and salinity values that range from 5.5 to 30.5 wt% NaCleq. (unpublished data from Guizhou Geological Bureau), consistent with the values of the SYG ore fluids (generally T_h < 200–250 °C and salinity values up to 22 wt% NaCleq.; Hu et al., 2017b; Wang et al., 2018; Zhang, 2006). These fluids are considered to have originated from basinal brine systems that are commonly associated with the formation of MVT deposits (Leach et al., 2005).

The currently available age data for the SYG deposits show a peak of Pb-Zn ore formation ranging from 230 to 190 Ma (Fig. 9), and the age of the Yunluheba deposit falls within this range, which indicates that they likely formed as a consequence of an intense hydrothermal event across the SYG area in the context of the Indosinian postorogenic uplift (Faure et al., 2014; Qiu et al., 2017; Wang et al., 2010). This event implies a topographically driven mechanism for fluid migration, which is interpreted to have occurred in most MVT deposits elsewhere in the world (Brannon et al., 1996a; Christensen et al., 1995; Leach et al., 2001; Nakai et al., 1993). Therefore, the Yunluheba Pb-Zn deposit, as well as other deposits in the SYG province, might have formed from the long-term migration of basinal brines driven by Indosinian postorogenic uplift. The Pb and Sr isotope data suggest that the ore sources were dominantly the host carbonates, possibly with some contribution from the basement. However, the Emeishan basalts show little relationship with the Yunluheba deposit. Therefore, the basinal brine might have extracted a large amount of metals (e.g., Pb and Zn) from wall rocks as they passed through during long-distance migration driven by Indosinian postcollisional elevated topography, and these brines eventually evolved into a metalliferous fluid. It might be interpreted by an alternate model (Fig. 11) that the Indosinian postorogenic uplift

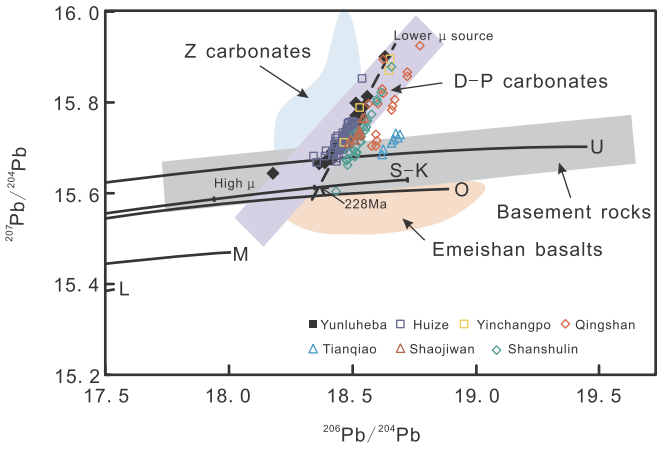

Fig. 8. Diagram of $^{207}Pb/^{204}Pb$ vs. $^{206}Pb/^{204}Pb$ for the Yunluheba deposit. Data for the plumbotectonic model are from Zartman and Doe (1981); average crustal Pb evolution is from Stacey and Krammers (1975, S-K). The data for the Huize deposit are from Huang et al. (2004); those for the Yinchangpo deposit are from Hu (1999); those for the Qingshan deposit are from Zhang et al. (1999) and Zhou et al. (2013e); those for the Shanshulin deposit are from Zhou et al. (2014a); those for the Tianqiao deposit are from Zhou et al. (2013d); and those for the Shaojiwan deposit are from Zhou et al. (2013b). The age-corrected isotopic ranges (200 Ma) for the Sinian (Z) Dengying Formation dolostone, the Devonian to Permian (D-P) carbonates, the Proterozoic basement rocks and the Emeishan basalts are delineated by the data from Zhou et al. (2014b). Abbreviations: U-upper crust, O-orogenic, M-mantle, and L-lower crust.

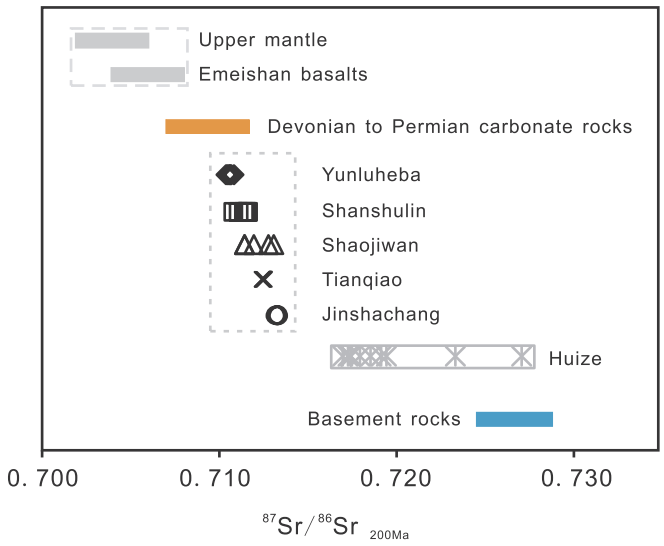

Fig. 10. Comparison of $^{87}Sr/^{86}Sr_{200Ma}$ ratios among the SYG Pb-Zn deposits, carbonate rocks, basement rocks, Emeishan basalts and upper mantle. The Sr isotope data are taken from Zhou et al. (2014a) for the Shanshulin deposit, from Zhou et al. (2013b) for the Shaojiwan deposit, from Zhou et al. (2013d) for the Tianqiao deposit, from Zhou et al. (2015) for the Jinshachang deposit and from Yin et al. (2009) for the Huize deposit. The Sr isotopic compositions of the reservoirs are all calculated back to 200 Ma with original data from Faure (1977) for the upper mantle; from Huang et al. (2004) for the Emeishan basalts; from Deng et al. (2000), Hu (1999), Zhou et al. (2014a) and Zhou et al. (2013b) for the sedimentary carbonates; and from Chen and Ran (1992) and Li and Qin (1988) for the Proterozoic basement rocks.

(~230–190 Ma) drove voluminous basinal brines to migrate through the basement and country rocks, where they extracted metals. The Yunluheba ore fluids acquired their metals mainly from the Devonian to Permian carbonate rocks. When the fluids were transported upward along a deep fault (e.g., the Yinchangpo-Yunluhe thrust fault in the Yunluheba area) into secondary faulting zones and encountered a resident H_2S-bearing fluid with homogeneously mixed sulfur produced by the alteration of synsedimentary pyrite and stratabound thermochemically reduced sulfate, the fluids precipitated sulfide minerals. Alternatively, the metalliferous fluids might bring in necessary heat that triggered a thermochemical reduction of sedimentary sulfates in country rocks in the presence of organic matter, which provided the reduced sulfur required for metal precipitation.

7. Conclusions

Our dating results suggest that the Yunluheba deposit formed at approximately 200 Ma, synchronously with many SYG Pb-Zn deposits, which indicates that their formation was related to an intense

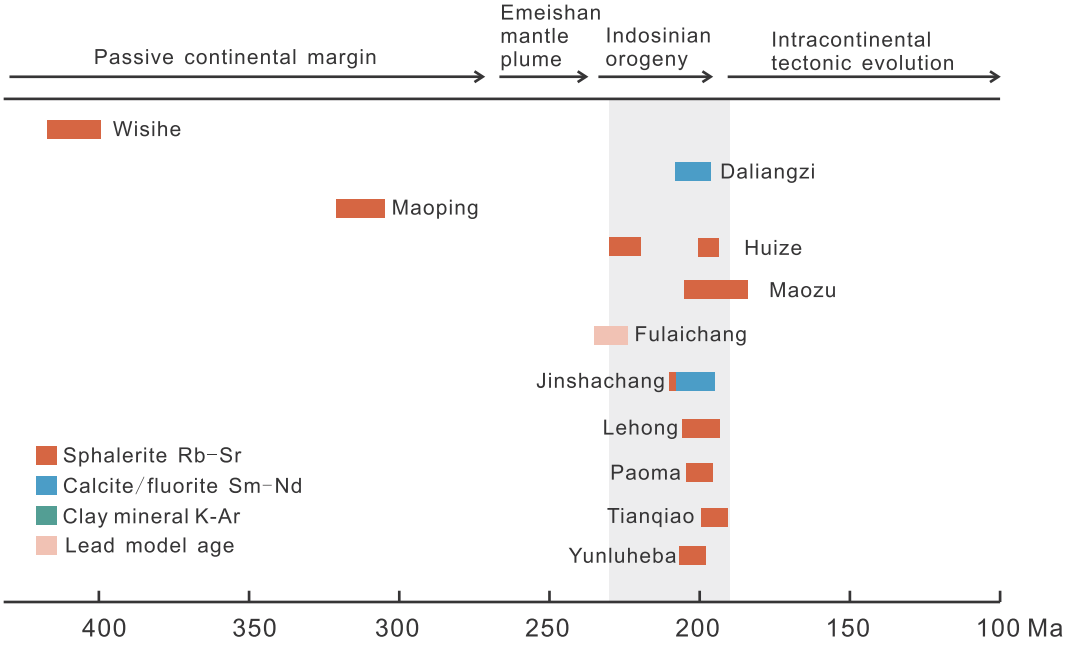

Fig. 9. Ages of some carbonate-hosted Pb-Zn deposits in the SYG metallogenic province and their corresponding geological settings (data from Lin et al., 2010; Shen et al., 2016; Yin et al., 2009; Zhang et al., 2014; Zhang et al., 2015; Zhou et al., 2013c; 2013d; Zhou et al., 2015; and this study).

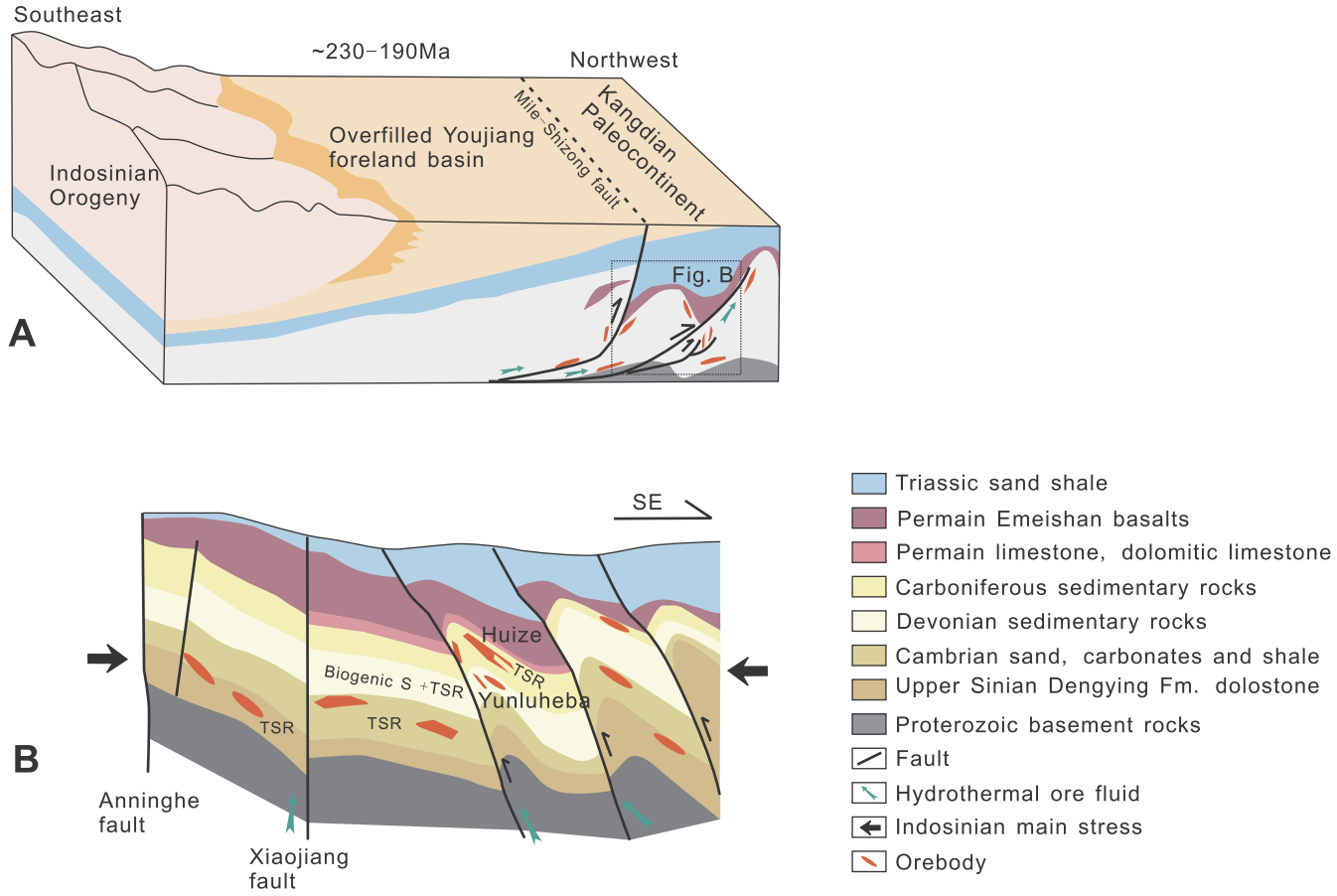

Fig. 11. A metallogenic model for the SYG Pb-Zn deposits related to the late Indosinian orogeny. A. The late Indosinian orogeny (~230–190 Ma), following the closure of the Paleo-Tethys ocean in the Middle Triassic, caused extensive topographic uplift, and the Youjiang area subsequently evolved into a foreland basin near the southern boundary of the SYG metallogenic province. Elevated topography drove voluminous basinal brines to migrate through the foreland basin and into the Kangdian paleocontinent (the site of the SYG Pb-Zn deposits) along deep faults (Zhang et al., 2015). These fluids extracted substantial metals from the country rocks and basement through which they passed, migrated upward and finally deposited at structurally favorable locations (e.g., anticline axes and interlayer fractures) when they met H_2S-bearing fluids. B. Upward-migrating metalliferous fluids were transported into secondary structures and precipitated sulfides when they encountered H_2S-bearing fluids generated by the mixing of synsedimentary pyrite alteration (biogenic S) and thermochemical sulfate reduction (TSR) in the Devonian strata (e.g., the Yunluheba deposit), and they may also have deposited in the strata (e.g., the Sinian, Cambrian, Carboniferous and Permian carbonates in the Huize, Daliangzi, Tianbaoshan and Qingshan deposits) where the H_2S was produced via TSR triggered by the heat introduced by hydrothermal fluids (modified after Zhou et al., 2015).

hydrothermal event throughout the SYG metallogenic province that occurred during the late Indosinian orogeny. Pb and Sr isotopic data suggest that the host carbonate rocks were the major source of metals, possibly with a small contribution from the basement. The sulfur isotopic variation in the Yunluheba deposit is interpreted to likely originate from the mixing of synsedimentary pyrite derived originally from biogenic sulfur and thermochemically reduced sulfur from seawater sulfates in the sedimentary successions. The low $\delta^{34}S$ values observed in the Devonian carbonate-hosted Pb-Zn deposits were constrained by the availability of synsedimentary pyrite in the host rocks rather than being a reflection of mantle-derived sulfur.

Declaration of Competing Interest

The authors declare that they have no known competing financial interests or personal relationships that could have appeared to influence the work reported in this paper.

Acknowledgments

This work was financially supported by the National Science Foundation of China (U1812402, 41703047, 41872095 and 41973047) and the Natural Science Foundation of Guizhou Province (2015-2141).

We thank two anonymous reviewers for their constructive comments that greatly helped improve the manuscript. We also thank the handling editor for handling this submission.

References

Bai, J.H., Huang, Z.L., Zhu, D., Yan, Z.F., Zhou, J.X., 2013. Isotopic compositions of sulfur in the Jinshachang lead-zinc deposit Yunnan, China. Acta Geol. Sin. (Engl. Ed.) 87, 1355–1369.

Basuki, N.I., Taylor, B.E., Spooner, E.T.C., 2008. Sulfur isotope evidence for thermochemical reduction of dissolved sulfate in Mississippi Valley-tye zinc-lead mineralization, Bongara area, northern Peru. Econ. Geol. 103, 783–799.

Bradley, D.C., Leach, D.L., Symons, D., Emsbo, P., Premo, W., Breit, G., Sangster, D.F., 2004. Reply to discussion on "Tectonic controls of Mississippi valley-type lead-zinc mineralization in orogenic forelands" by S.E. Kesler, J.T. Christensen, R.D. Hagni, W. Heijlen, J.R. Kyle, K.C. Misra, P. Muchez, and R. van der Voo Mineralium Deposita. Mineralium Deposita 39, 515–519.

Brannon, J.C., Cole, S.C., Podosek, F.A., Ragan, V.M., Coveney, R.M., Wallace, M.W., Bradley, A.J., 1996a. Th-Pb and U-Pb dating of ore-stage calcite and paleozoic fluid flow. Science 271, 491–493.

Brannon, J.C., Podosek, F.A., Cole, S.C., 1996b. Radiometric dating of Mississippi Valley-type ore deposits. Carbonate-Hosted Lead-zinc Deposit. Soc Econ Geol Special Publ.

Cao, L., Duan, Q.F., Zhou, Y., 2015. Rb-Sr dating of sphalerites from the Aozigang zinc deposit in Hubei Province and its geological significance. Geol. China 42, 235–247 (in Chinese with English abstract).

Chaussidon, M., Albarede, F., Sheppard, S.M.F., 1989. sulfur isotope variations in the mantle from ion microprobe analyses of micro-sulfide inclusions. Earth Planet. Sc. Lett. 92, 144–156.

Chen, H.S., Ran, C.Y., 1992. Geochemistry of Copper Deposit in Kangdian area. Geological Publishing House, Beijing.
Christensen, J.N., Halliday, A.N., Vearncombe, J.R., Kesler, S.E., 1995. Testing models of large-scale crustal fluid-flow using direct dating of sulfides – RB-SR evidence for early dewatering and formation of mississippi valley-type deposits, Canning Basin, Australia. Econ. Geol. Bull. Soc. Econ. Geol. 90, 877–884.
Deng, H.L., Li, C.Y., Tu, G.Z., Zhou, Y.M., Wang, C.W., 2000. Strontium isotope geochemistry of the Lemachang independent silver ore deposit, northeastern Yunnan. China. Sci. China Ser. D Earth Sci. 43, 337–346.
Deng, P., Yang, G., 2015. Genetic model and prospecting potential for the Maoping-Yunluheba-Dafa Pb-Zn ore field. Sichuan Geological Sinica 35, 351–354 (in Chinese with English abstract).
Dostal, J., Capedri, S., 1978. Uranium in metamorphic rocks. Contrib. Mineral. Petrol. 66, 409–414.
Downes, H., Markwick, A.J.W., Kempton, P.D., Thirlwall, M.F., 2001. The lower crust beneath cratonic north-east Europe: isotopic constraints from garnet granulite xenoliths. Terra Nova 13, 395–400.
Faure, G., 1977. Principles of Isotope Geology. John Wiley & Sons, New York, pp. 28–110.
Faure, G., Mensing, T.M., 2005. Isotopes: Principles and Applications (3rd edition). John Wiley & Sons, New Jersey, pp. 256–283.
Faure, M., Lepvrier, C., Vuong Van, N., Tich Van, V., Lin, W., Chen, Z., 2014. The South China block-Indochina collision: where, when, and how? J. Asian Earth Sci. 79, 260–274.
Feng, C.X., Liu, S., Bi, X.W., Hu, R.Z., Chi, G.X., Chen, J.J., Feng, Q., Guo, X.L., 2017. An investigation of metallogenic chronology of eastern ore block in Baiyangping Pb-Zn-Cu-Ag polylmetallic ore deposit, Lanping Basin, western Yunnan Province. Mineral Deposits 36, 691–704 (in Chinese with English abstract).
Franklin, J.M., 1983. Lead isotope studies in Superior and Southern Provinces. Bull. Geol. Survey Canada 351, 1–35.
Gao, S., Ling, W.L., Qiu, Y.M., Lian, Z., Hartmann, G., Simon, K., 1999. Contrasting geochemical and Sm-Nd isotopic compositions of Archean metasediments from the Kongling high-grade terrain of the Yangtze craton: evidence for cratonic evolution and redistribution of REE during crustal anatexis. Geochim. Cosmochim. Acta 63, 2071–2088.
Han, R.S., Liu, C.Q., Huang, Z.L., Chen, J., Ma, D.Y., Lei, L., Ma, G.S., 2007. Geological features and origin of the Huize carbonate-hosted Zn–Pb–(Ag) District, Yunnan, South China. Ore Geol. Rev. 31, 360–383.
Hei, H.X., Su, S.G., Wang, Y., Mo, X.X., Liu, W.G., 2018. Rhyolites in the Emeishan large igneous province (SW China) with implications for plume-related felsic magmatism. J. Asian Earth Sci. 164, 344–365.
Hu, R.Z., Chen, T.W., Xu, D.R., Zhou, M.-F., 2017a. Reviews and new metallogenic models of mineral deposits in South China: an introduction. J. Asian Earth Sci. 137, 1–8.
Hu, R.Z., Fu, S., Huang, Y., Zhou, M.-F., Fu, S., Zhao, C., Wang, Y., Bi, X., Xiao, J., 2017b. The giant South China Mesozoic low-temperature metallogenic domain: reviews and a new geodynamic model. J. Asian Earth Sci. 137, 9–34.
Hu, Y.G., 1999. Ag occurrence, source of ore-forming metals and mechanism of Yinchangpo Ag-Pb-Zn deposit, Guizhou. Institute of Geochemistry, CAS, pp. 10–55 (in Chinese with English abstract).
Huang, Z.L., Chen, J., Han, R.S., 2004. Geochemistry and Ore-formation of the Huize Giant Lead-zinc Deposit, Yunnan Province, China: Discussion on the Relationship Between the Emeishan Flood Basalts and Lead-zinc Mineralization. Geological Publishing House, Beijing.
Jia, D., Wei, G.Q., Chen, Z.X., Li, B.Q., Zeng, Q., Yang, G., 2006. Longmen Shan fold-thrust belt and its relation to the western Sichuan Basin in central China: new insights from hydrocarbon exploration. AAPG Bull. 90 (9), 1425–1447.
Jin, X.L., Meng, C.Z., Leng, C.B., Qi, Y.Q., Tang, Y.Y., Zhang, H., Chen, X., 2016. Element geochemical characteristics and C-O isotopic compositions of Pb-Zn deposit in Yunluheba area of Guizhou and their geological implications. J. Earth Sci. Environ. 38, 778–780 (in Chinese with English abstract).
Jin, Z.G., Huang, Z.L., 2008. Study on ore-controlling factors of Pb-Zn deposits and prospecting model in the area of southwestern Guizhou. Acta Mineralogica Sinica 28, 467–472 (in Chinese with English abstract).
Kiyosu, Y., 1980. Chemical-reduction and sulfur-isotope effects of sulfate by organic-matter under hydrothermal conditions. Chem. Geol. 30, 47–56.
Kong, Z.G., Wu, Y., Zhang, F., Zhang, C.Q., Meng, X.Y., 2018. Sources of ore-forming material of typical Pb-Zn deposits in the Sichuan-Yunnan-Guizhou metallogenic province: constraints from the S-Pb isotopic compositions. Earth Sci. Front. 25, 125–137 (in Chinese with English abstract).
Leach, D.L., Dwight, B., Lewchuk, M.T., Symons, D.T.A., de Marsily, G., Brannon, J., 2001. Mississippi Valley-type lead-zinc deposits through geological time: implications from recent age-dating research. Miner. Deposita 36, 711–740.
Leach, D.L., Sangster, D.F., 1993. Mississippi Valley-type lead-zinc deposits. In: Kirkham, R.V. (Eds), Mineral Deposit models. Geol. Assoc. Can. Spec. Pap., pp. 289–314.
Leach, D.L., Sangster, D.F., Kelley, K.D., Larger, R.R., Garven, G., Allen, C.R., Gutzmer, J., Walters, S., 2005. Sediment-hosted zinc-lead deposits: a global perspective. Economic Geology 100th Anniversary Volume, 561–607.
Li, C.Y., 1999. Some geological characteristics of concentrated distribution area of epithermal deposits in China. Earth Sci. Front 6, 163–170 (in Chinese with English abstract).
Li, F.H., Qin, J.M., 1988. Presinian System in Kangdian Area. Chongqing Press, Chongqing.
Li, F.Y., 2003. Study on occurrence state and enrichment mechanism of dispersed elements in MVT deposits—a case study for the Tianbaoshan and Daliangzi Pb-Zn deposits in Sichuan Province. Chengdu University of Technology, Chengdu, pp. 35–37 (in Chinese with English abstract).
Li, W., Huang, Z.L., Yin, M., 2007. Dating of the giant Huize Zn-Pb ore field of Yunnan Province, Southwest China: constraints from the Sm-Nd system in hydrothermal calcite. Resour. Geol. 57, 90–97.
Li, W.B., Huang, Z.L., Wang, Y.X., Chen, J., Han, R.S., Xu, C., Guan, T., Yin, M.D., 2004. Ages of the giant Huize Zn-Pb deposits determined by Sm-Nd dating of hydrothermal calcite. Geol. Rev. 50, 189–195 (in Chinese with English abstract).
Li, X.B., Huang, Z.L., Li, W.B., Zhang, Z.L., Yan, Z.F., 2006. Sulfur isotopic compositions of the Huize super-large Pb-Zn deposit, Yunnan Province, China: implications for the source of sulfur in the ore-forming fluids. J. Geochem. Explor. 89, 227–230.
Liang, F., 2017. Metallogenesis of the lead-zinc deposit in Chuan-Dian-Qian district: Case study of the Tianbaoshan, Fule, Shanshulin Pb-Zn deposit. University of Chinese Academy of Sciences, Guiyang.
Liao, W., 1984. Sulfur isotopic compositions and the ore model of the Pb-Zn deposits in the eastern Yunnan and western Guizhou areas Geology and Exploration 1, 2–6 (in Chinese).
Liao, Z.W., Deng, X.W., 2002. Geological structural and characteristic in Yinchangpo Pb-Zn-Ag deposits and its prospecting analysis. Guizhou Geol. 19, 163–168 (in Chinese with English abstract).
Lin, Z.Y., Wang, D.H., Zhang, C.Q., 2010. Rb-Sr isotopic age of sphalerite from the Paoma lead-zinc deposit in Sichuan Province and its implications. Geol. China 37, 488–1196 (in Chinese with English abstract).
Liu, H.C., Lin, W.D., 1999. Study of the Pb-Zn-Ag metallogenic regularity in the Northeastern Yunnan Province. Yunnan University Publisher, China, Kunming in Chinese.
Liu, H.Y., Xia, B., Zhang, Y.Q., 2004. SHRIMP dating of zircon from Maomaogou agpatic alkalic rocks in Huili County, Panxi, and its geological implications. China Sci. Bull. 49, 1431–1438 (in Chinese).
Liu, J.M., Zhao, S.R., Shen, J., Jiang, N., Huo, W.G., 1998. Review on direct isotopic dating of hydrothermal ore-forming processes. Progr. Geophys. 13, 46–55 (in Chinese with English abstract).
Liu, W.H., Zhang, J., Wang, J., 2017. Sulfur isotope analysis of carbonate-hosted Zn–Pb deposits in northwestern Guizhou Province, Southwest China: implications for the source of reduced sulfur. J. Geochem. Explor. 181, 31–44.
Lu, S.S., Qiu, X.F., Tan, J.J., Lv, H., Yang, H.M., Wang, X.Z., Zhong, Q., 2016. The Pb-Pb isochron age of the Kuangshishan Formation in Shennongjia area on the Northern margin of the Yangtze Craton and its geological implications. Earth Sci. 42, 317–324 (in Chinese with English abstract).
Ludwig, R.K., 2005. Isoplot/EX rev. 3.32: a geochronological toolkit for Microsoft Excel. Berkeley Geochronology Center, Special Publication 4, Berkeley, pp. 1–71.
Luo, K., Zhou, J.X., Huang, Z.L., Wang, X.C., Wilde, S., Zhou, W., Tian, L.Y., 2019. New insights into the origin of early Cambrian carbonate-hosted Pb-Zn deposits in South China: a case study of the Maliping Pb-Zn deposit. Gondwana Res. 70, 88–103.
Machel, H.G., 2001. Bacterial and thermochemical sulfate reduction in diagenetic settings: old and new insights. Sed. Geol. 140, 143–175.
Maluski, H., Lepvrier, C., Jolivet, L., Carter, A., Roques, D., Beyssac, O., Nguyen, D.T., Ta, T.T., Avigad, D., 2001. Ar-Ar and fission track ages in the Song Chay massif: early Triassic and Cenozoic tectonics in northern Vietnam. J. Asian Earth Sci. 19, 233–248.
Mirnejad, H., Simonetti, A., Molasalehi, F., 2011. Pb isotopic compositions of some Zn–Pb deposits and occurrences from Urumieh-Dokhtar and Sanandaj-Sirjan zones in Iran. Ore Geol. Rev. 39, 181–187.
Nakai, S., Halliday, A.N., Kesler, S.E., Jones, H.D., 1990. RB-SR dating of sphalerites from Tennessee and the genesis of Mississippi valley type ore-deposits. Nature 346, 354–357.
Nakai, S.i., Halliday, A.N., Kesler, S.E., Jones, H.D., Kyle, J.R., Lane, T.E., 1993. Rb-Sr dating of sphalerites from Mississippi Valley-type (MVT) ore deposits. Geochim. Cosmochim. Acta 57, 417–427.
Nelson, J., Paradis, S., Christensen, J., Gabites, J., 2002. Canadian Cordilleran Mississippi Valley-type deposits: a case for Devonian-Mississippian back-arc hydrothermal origin. Econ. Geol. Bull. Soc. Econ. Geol. 97, 1013–1036.
Ohmoto, H., 1986. Stable isotopes in high temperature geological process. Rev. Mineral. Geochem. Mineral. Soc. Am. 16, 491–559.
Ohmoto, H., Rye, R.O., 1979. Isotopes of sulfur and carbon, second ed. Wiley, New York.
Ostendorf, J., Henjes-Kunst, F., Schneider, J., Melcher, F., Gutzmer, J., 2017. Genesis of the carbonate-hosted tres marias Zn-Pb-(Ge) deposit, Mexico: constraints from Rb-Sr sphalerite geochronology and Pb isotopes. Econ. Geol. 112, 1075–1087.
Pettke, T., Diamond, L.W., 1995. RB-SR isotopic analysis of fluid inclusions in quartz-evaluation of bulk extraction procedures and geochronometer systematics using synthetic fluid inclusions. Geochim. Cosmochim. Acta 59, 4009–4027.
Qiu, L., Yan, D.-P., Yang, W.-X., Wang, J., Tang, X., Ariser, S., 2017. Early to Middle Triassic sedimentary records in the Youjiang Basin, South China: implications for Indosinian orogenesis. J. Asian Earth Sci. 141, 125–139.
Qiu, Y.M.M., Gao, S., 2000. First evidence of > 3.2 Ga continental crust in the Yangtze craton of South China and its implications for Archean crustal evolution and Phanerozoic tectonics. Geology 28, 11–14.
Rosa, D., Schneider, J., Chiaradia, M., 2016. Timing and metal sources for carbonate-hosted Zn-Pb mineralization in the Franklinian Basin (North Greenland): constraints from Rb-Sr and Pb isotopes. Ore Geol. Rev. 79, 392–407.
Sangster, D.F., 1996. Mississippi Valley-type lead-zinc. Geological Survey of Canada.
Schneider, J., Haack, U., Stedingk, K., 2003. Rb-Sr dating of epithermal vein mineralization stages in the eastern Harz Mountains (Germany) by paleomixing lines. Geochim. Cosmochim. Acta 67, 1803–1819.
Schneider, J., Melcher, F., Brauns, M., 2007. Concordant ages for the giant Kipushi base metal deposit (DR Congo) from direct Rb-Sr and Re-Os dating of sulfides. Miner. Deposita 42, 791–797.
Sebastian Staude, S.G., Pfaff, Katharina, Ströbele, Florian, Premo, Wayne R., Markl, Gregor, 2011. Deciphering fluid sources of hydrothermal systems: a combined Sr- and S-isotope study on barite (Schwarzwald, SW Germany). Chem. Geol. 286, 1–20.

Shen, Z.W., Jin, C.H., Dai, Y.P., Zhang, Y., Zhang, H., 2016. Mineralization Age of the Maoping Pb-Zn Deposit in the Northeastern Yunnan Province: evidence from Rb-Sr Isotopic Dating of Sphalerites. Geol. J. China Universities 22, 213–218 (in Chinese with English abstract).
Si, R.J., Gu, X.X., Xie, L.X., Zhang, N., 2013. Geological characteristics of the Fule polymetallic deposit in Yunnan Province: a Pb-Zn deposit with dispersed elements and unusual enrichment. Geol. Explor. 29, 313–322 (in Chinese with English abstract).
Stacey, J., Krammers, J., 1975. Approximation terrestrial lead isotope evolution by a two-stage mode. Earth Planet. Sci. Lett. 26, 207–221.
Sun, W.-H., Zhou, M.-F., Gao, J.-F., Yang, Y.-H., Zhao, X.-F., Zhao, J.-H., 2009. Detrital zircon U-Pb geochronological and Lu-Hf isotopic constraints on the Precambrian magmatic and crustal evolution of the western Yangtze Block, SW China. Precambr. Res. 172, 99–126.
Tang, H.S., 1999. Report on the ore-forming environment, regularity and exploration predict for the Au, Ag, Pb and Zn deposits in the adjacent area of the Yunnan, Guizhou and Guangxi Provinces. Institute of Guilin Mineral Geology Research, Guilin.
Tang, Y., Bi, X., Fayek, M., Stuart, F.M., Wu, L., Jiang, G., Xu, L., Liang, F., 2017. Genesis of the Jinding Zn-Pb deposit, northwest Yunnan Province, China: constraints from rare earth elements and noble gas isotopes. Ore Geol. Rev.
Tian, S.H., Y.L., G., Yang, Z.S., Hou, Z.Q., Liu, Y.C., Song, Y.C., Xue, W.W., Lu, H.F., Wang, F.C., Zhang, Y.B., Zhu, T., Yu, C.J., 2014. Rb-Sr and Sm-Nd isochron ages of the dongmozhazhua and mohailaheng Pb-Zn Ore deposits in the Yushu area, southern Qinghai and Their Geological Implicatio. Acta Geologica Sinica (English Edition) 88, 558–569.
Tu, G.C., 1998. The Low Temperature Geochemistry. Science Press, Beijing (in Chinese).
Wang, J., Zhang, J., Zhong, W.B., Yang, Q., Li, F.K., Zhu, Z.K., 2018. Sources of ore-forming fluids from Tianbaoshan and Huize carbonate-hosted Pb-Zn deposits in Yunnan-Sichuan-Guizhou region, Southwestern China. Earth Sci.
Wang, J.Z., Li, C.Y., Li, Z.Q., Liu, J.J., 2001. The geological setting, characters and origin of Mississippi Valley-type Pb-Zn deposits in Sichuan and Yunnan provinces. Geol.-Geochem. 29, 41–45.
Wang, Q., Gu, X.X., Fu, S.H., Zhang, M., Li, F.Y., 2008. Enrichment of the dispersed elements Cd, Ge and Ga in the Huize lead-zinc deposit, Yunnan. Sediment. Geol. Tethyan Geol. 28, 69–73 (in Chinese with English abstract).
Wang, R., Zhang, C.Q., Wu, Y., Wei, C., 2012. Formation age of the diabase dike in the Tianbaoshan Pb-Zn deposit, Sichuan and its relationships with the Pb-Zn mineralization. Mineral Deposits 31, 449–450 (in Chinese).
Wang, W., Zhou, M.F., Zhao, X.F., Chen, W.T., Yan, D.P., 2014. Late Paleoproterozoic to Mesoproterozoic rift successions in SW China: Implication for the Yangtze Block-North Australia-Northwest Laurentia connection in the Columbia supercontinent. Sed. Geol. 309, 33–47.
Wang, X.C., 1991. Genesis analysis of Daliangzi Pb-Zn deposit in Sichuan province. Miner. Resour. Geol. 5, 151–156 (in Chinese with English abstract).
Wang, X.C., 1992. Genesis analysis of the Tianbaoshan Pb-Zn deposit. J. Chengdu Coll. Geol. 19, 10–20 (in Chinese with English abstract).
Wang, Y., Zhang, A., Fan, W., Peng, T., Zhang, F., Zhang, Y., Bi, X., 2010. Petrogenesis of late Triassic post-collisional basaltic rocks of the Lancangjiang tectonic zone, southwest China, and tectonic implications for the evolution of the eastern Paleotethys: Geochronological and geochemical constraints. Lithos 120, 529–546.
Wang, Y.X., Yang, J.D., Chen, J., Zhang, K.J., Rao, W.B., 2007. The Sr and Nd isotopic variations of the Chinese Loess Plateau during the past 7 Ma: implications for the East Asian winter monsoon and source areas of loess. Palaeogeogr. Palaeoclimatol. Palaeoecol. 249, 351–361.
Wang, Y.X., Yang, J.D., Tao, X.C., Li, H.M., 1988. The study of the Sm-Nd method for fossil mineral rock and its application. J. Nanjing University 24, 297–308 (in Chinese with English abstract).
Warren, J.K., 1999. Evaporites: Their Evolution and Economics. Blackwell Scientifific, Oxford, UK, pp. 438.
Wu, Y., 2013. The age and ore-forming process of MVT deposits in the boundary area of Sichuan-Yunnan-Guizhou provinces, Southwest China. China University of Geosciences, Beijing, pp. 1–167 (in Chiese with English abstract).
Xia, B., Liu, H.Y., Zhang, Y.Q., 2004. SHRIMP dating of agpaitic alkalic rocks in Panxi rift zone and its geological implications—examples for Hongge, Baima and Jijie rock bodies. Geotectonica et Metallogenia 28, 149–154 (in Chinese with English abstract).
Xiong, S.-F., Gong, Y.-J., Jiang, S.-Y., Zhang, X.-J., Li, Q., Zeng, G.-P., 2018. Ore genesis of the Wusihe carbonate-hosted Zn-Pb deposit in the Dadu River Valley district, Yangtze Block, SW China: evidence from ore geology, S-Pb isotopes, and sphalerite Rb-Sr dating. Miner. Deposita 1432–1866.
Xu, Y., Huang, Z., Zhu, D., Luo, T., 2014. Origin of hydrothermal deposits related to the Emeishan magmatism. Ore Geol. Rev. 63, 1–8.
Xu, Y.G., Chung, S.L., Jahn, B.M., 2001. Petrologic and geochemical constraints on the petrogenesis of Permian-Triassic Emeishan flood basalts in southwestern China. Lithos 58, 145–168.
Yan, D.P., Zhou, M., Wang, C.Y., Xia, B., 2006. Structural and geochronological constraints on the tectonic evolution of the Dulong-Song Chay tectonic dome in Yunnan province, SW China. J. Asian Earth Sci. 28, 332–353.
Yang, N.W., 2015. Discussion on the exploration perspect of Pb-Zn-Ag deposits in the Yinchangpo-Yunluhe area in Weining County. Guizhou Province Western-China Exploration Engineering 143–149 (in Chinese).
Yang, J.H., Cawood, P.A., Du, Y.S., Huang, H., Hu, L.S., 2012. Detrital record of Indosinian mountain building in SW China: provenance of the Middle Triassic turbidites in the Youjiang Basin. Tectonophysics 574, 105–117.
Yang, X.Y., Zhou, J.X., An, Q., Ren, H.Z., Xu, L., Lu, M.D., Wu, C.J., 2018. Formation mechanism of reduced S in the Nayongzhi Pb-Zn deposit, Guizhou province, China: constraint from the NanoSIMS in-situ S isotopes. Acta Mineralogica Sinica 38, 593–599 (in Chinese with English abstract).
Yin, M.D., Li, W.B., Sun, X.W., 2009. Rb-Sr isotopic dating of sphalerite from the giant Huize Zn-Pb ore field, Yunnan Province, Southwestern China. Chin. J. Geochem. 28, 70–75.
Yong, L., Allen, P.A., Densmore, A.L., Qiang, X., 2003. Evolution of the Longmen Shan foreland basin (western Sichuan, China) during the Late Triassic Indosinian orogeny. Basin Res. 15 (1), 117–138.
Zartman, R.E., Doe, B.R., 1981. Plumbotyectonics-the mode. Tectonophysics 75, 135–162.
Zaw, K., Peters, S.G., Cromie, P., Burrett, C., Hou, Z., 2007. Nature, diversity of deposit types and metallogenic relations of South China. Ore Geol. Rev. 31, 3–47.
Zhang, C., Wu, Y., Hou, L., Mao, J., 2015. Geodynamic setting of mineralization of Mississippi Valley-type deposits in world-class Sichuan–Yunnan–Guizhou Zn–Pb triangle, southwest China: implications from age-dating studies in the past decade and the Sm–Nd age of Jinshachang deposit. J. Asian Earth Sci. 103, 103–114.
Zhang, C.Q., Li, X.H., Yu, J.J., Mao, J.W., Chen, F.K., Li, H.M., 2008. Rb-Sr Dating of Single Sphalerites from the Daliangzi Pb-Zn Deposit, Sichuan, and Its Geological Signif icances. Geol. Rev. 54, 532–538 (in Chinese with English abstract).
Zhang, H., Meng, C.Z., Qi, Y.Q., Tang, Y.Y., Jin, X.L., Chen, X., Leng, C.B., 2016. Sources of the ore-forming materials from Yunheheba ore field in Northwest Guizhou province, China: constraints from S and Pb isotope geochemistry. Acta Mineralogica Sinica 36, 271–276 (In Chinese with English abstract).
Zhang, Q.H., Gu, S.Y., Mao, J.Q., 1999. Geochemical study on Qingshan lead-zinc deposit in Shuicheng, Guizhou Province. Geol.-Geochem. 27, 15–20 (in Chinese with English abstract).
Zhang, Y.X., Wu, Y., Tian, G., Shen, L., Zhou, Y.M., Dong, W.W., Zeng, R., Yang, X.C., Zhang, C.Q., 2014. Mineralization age and the source of ore-forming material at Lehong Pb-Zn deposit, Yunnan province: constraints from Rb-Sb and S isotopes system. Acta Mineralogica Sinica 34, 305–411 (in Chinese with English abstract).
Zhang, Z.L., 2006. Feature and sources of ore-forming fluid in the Huize lead-zinc ore deposits, Yunnan province, China: evidence from fluid inclusions and water-rock reaction experiments. Institute of Geochemistry, Chinese Academy of Sciences, Guizyang, pp. 23–31 (in Chinese with English abstract).
Zhao, X.F., Zhou, M.F., Li, J.F., Sun, M., Gao, J.F., Sun, W.H., Yang, J.H., 2010. Late Paleoproterozoic to early Mesoproterozoic Dongchuan Group in Yunnan, SW China: implications for tectonic evolution of the Yangtze Block. Precambr. Res. 182, 57–69.
Zhao, Z., 1995. Genetic models for the Pb-Zn deposits in the eastern and noetheastern Yunnan areas. Yunnan Geol. 14, 350–354 (in Chinese).
Zheng, M.H., Wang, X.C., 1991. Genesis of the Daliangzi Pb-Zn deposit in Sichuan, China. Econ. Geol. Bull. Soc. Econ. Geol. 86, 831–846.
Zhong, H., Campbell, I.H., Zhu, W.G., Allen, C.M., Hu, R.Z., Xie, L.W., He, D.F., 2011. Timing and source constraints on the relationship between mafic and felsic intrusions in the Emeishan large igneous province. Geochim. Cosmochim. Acta 75, 1374–1395.
Zhou, C.X., Wei, C.S., Guo, J.Y., Li, C.Y., 2001. The source of metals in the Qilinchang Zn-Pb deposit, northeastern Yunnan, China: Pb-Sr isotope constraints. Econ. Geol. Bull. Soc. Econ. Geol. 96, 583–598.
Zhou, J.-X., Gao, J.-G., Chen, D., Liu, X.-K., 2013a. Ore genesis of the Tianbaoshan carbonate-hosted Pb-Zn deposit, Southwest China: geologic and isotopic (C-H-O-S-Pb) evidence. Int. Geol. Rev. 55, 1300–1310.
Zhou, J.-X., Huang, Z.-L., Lv, Z.-C., Zhu, X.-K., Gao, J.-G., Mirnejad, H., 2014a. Geology, isotope geochemistry and ore genesis of the Shanshulin carbonate-hosted Pb–Zn deposit, southwest China. Ore Geol. Rev. 63, 209–225.
Zhou, J.-X., Huang, Z.-L., Zhou, M.-F., Zhu, X.-K., Muchez, P., 2014b. Zinc, sulfur and lead isotopic variations in carbonate-hosted Pb–Zn sulfide deposits, southwest China. Ore Geol. Rev. 58, 41–54.
Zhou, J.-X., Luo, K., Wang, X.-C., Wilde, S.A., Wu, T., Huang, Z.-L., Cui, Y.-L., Zhao, J.-X., 2018a. Ore genesis of the Fule PbZn deposit and its relationship with the Emeishan Large Igneous Province: evidence from mineralogy, bulk COS and in situ SPb isotopes. Gondwana Res. 54, 161–179.
Zhou, J.-X., Xiang, Z.-Z., Zhou, M.-F., Feng, Y.-X., Luo, K., Huang, Z.-L., Wu, T., 2018b. The giant Upper Yangtze Pb–Zn province in SW China: reviews, new advances and a new genetic model. J. Asian Earth Sci. 154, 280–315.
Zhou, J., Huang, Z., Bao, G., 2013b. Geological and sulfur–lead–strontium isotopic studies of the Shaojiwan Pb–Zn deposit, southwest China: implications for the origin of hydrothermal fluids. J. Geochem. Explor. 128, 51–61.
Zhou, J., Huang, Z., Yan, Z., 2013c. The origin of the Maozu carbonate-hosted Pb–Zn deposit, southwest China: constrained by C-O–S–Pb isotopic compositions and Sm–Nd isotopic age. J. Asian Earth Sci. 73, 39–47.
Zhou, J., Huang, Z., Zhou, M., Li, X., Jin, Z., 2013d. Constraints of C-O–S–Pb isotope compositions and Rb–Sr isotopic age on the origin of the Tianqiao carbonate-hosted Pb–Zn deposit, SW China. Ore Geol. Rev. 53, 77–92.
Zhou, J.X., Bai, J.H., Huang, Z.L., Zhu, D., Yan, Z.F., Lv, Z.C., 2015. Geology, isotope geochemistry and geochronology of the Jinshachang carbonate-hosted Pb-Zn deposit, southwest China. J. Asian Earth Sci. 98, 272–284.
Zhou, J.X., Huang, Z.L., Gao, J.G., Yan, Z.F., 2013e. Geological and C-O-S-Pb-Sr isotopic constraints on the origin of the Qingshan carbonate-hosted Pb-Zn deposit, Southwest China. Int. Geol. Rev. 55, 904–916.
Zhou, J.X., Huang, Z.L., Zhou, G.F., Li, X.B., Ding, W., Bao, G.P., 2011. Trace elements and rare earth elements of sulfide minerals in the tianqiao Pb-Zn ore deposit, Guizhou Province, China. Acta Geologica Sinica-English Edition 85, 189–199.
Zhou, J.X., Wang, X.C., Wilde, S.A., Luo, K., Huang, Z.L., Wu, T., Jin, Z.G., 2018c. New insights into the metallogeny of MVT Zn-Pb deposits: A case study from the Nayongzhi in South China, using field data, fluid compositions, and in situ S-Pb isotopes. Am. Mineral. 103, 91–108.
Zhou, M.-F., Malpas, J., Song, X.-Y., Robinson, P.T., Sun, M., Kennedy, A.K., Lesher, C.M.,

Keays, R.R., 2002. A temporal link between the Emeishan large igneous province (SW China) and the end-Guadalupian mass extinction. Earth Planet. Sci. Lett. 196, 113–122.
Zhu, C., Liao, S., Wang, W., Zhang, Y., Yang, T., Fan, H., Wen, H., 2018. Variations in Zn and S isotope chemistry of sedimentary sphalerite, Wusihe Zn-Pb deposit, Sichuan Province, China. Ore Geol. Rev. 95, 639–648.
Zhu, L.Y., Su, W.C., Shen, N.P., Dong, W.D., Cai, J.L., Zhang, Z.W., Zhao, H., Xie, P., 2016. Fluid inclusion and sulfur isoopic studies of lead-zinc deposits, northwesern Guizhou, China. Acta Petrologica Sinica 32, 3431–3440 (in Chinese wih English abstract).